



OPEN ACCESS

Edited by:

Lavinia Alberi,
SICHH, Switzerland

Reviewed by:

Johnathan Cooper-Knock,
University of Sheffield,
United Kingdom
Paul Roy Heath,
University of Sheffield,
United Kingdom

***Correspondence:**

Eva L. Feldman
efeldman@umich.edu

† Present address:

Ximena Paez-Colasante,
Department of Biochemistry and
Biophysics, Interdisciplinary Graduate
Program in Genetics, Texas A & M
University, College Station, TX, USA
Carey Backus,
AbbVie Biotherapeutics Corporation,
Redwood City, CA, USA
Laurie Heinicke,
Medtronic Inc., Santa Rosa, CA, USA

Specialty section:

This article was submitted to Cellular
Neuropathology, a section of the
journal *Frontiers in Cellular
Neuroscience*

Received: 14 February 2020

Accepted: 14 April 2020

Published: 12 May 2020

Citation:

Paez-Colasante X,
Figuroa-Romero C, Rumora AE,
Hur J, Mendelson FE, Hayes JM,
Backus C, Taubman GF, Heinicke L,
Walter NG, Barmada SJ,
Sakowski SA and Feldman EL
(2020) Cytoplasmic TDP43 Binds
microRNAs: New Disease Targets in
Amyotrophic Lateral Sclerosis.
Front. Cell. Neurosci. 14:117.
doi: 10.3389/fncel.2020.00117

Cytoplasmic TDP43 Binds microRNAs: New Disease Targets in Amyotrophic Lateral Sclerosis

Ximena Paez-Colasante^{1†}, Claudia Figuroa-Romero¹, Amy E. Rumora¹, Junguk Hur², Faye E. Mendelson¹, John M. Hayes¹, Carey Backus^{1†}, Ghislaine F. Taubman¹, Laurie Heinicke^{3†}, Nils G. Walter³, Sami J. Barmada¹, Stacey A. Sakowski¹ and Eva L. Feldman^{1*}

¹Department of Neurology, University of Michigan, Ann Arbor, MI, United States, ²Department of Biomedical Sciences, School of Medicine and Health Sciences, University of North Dakota, Grand Forks, ND, United States, ³Single Molecule Analysis Group, Department of Chemistry, University of Michigan, Ann Arbor, MI, United States

Amyotrophic lateral sclerosis (ALS) is a progressive, fatal, and incurable neurodegenerative disease. Recent studies suggest that dysregulation of gene expression by microRNAs (miRNAs) may play an important role in ALS pathogenesis. The reversible nature of this dysregulation makes miRNAs attractive pharmacological targets and a potential therapeutic avenue. Under physiological conditions, miRNA biogenesis, which begins in the nucleus and includes further maturation in the cytoplasm, involves trans-activation response element DNA/RNA-binding protein of 43 kDa (TDP43). However, TDP43 mutations or stress trigger TDP43 mislocalization and inclusion formation, a hallmark of most ALS cases, that may lead to aberrant protein/miRNA interactions in the cytoplasm. Herein, we demonstrated that TDP43 exhibits differential binding affinity for select miRNAs, which prompted us to profile miRNAs that preferentially bind cytoplasmic TDP43. Using cellular models expressing TDP43 variants and miRNA profiling analyses, we identified differential levels of 65 cytoplasmic TDP43-associated miRNAs. Of these, approximately 30% exhibited levels that differed by more than 3-fold in the cytoplasmic TDP43 models relative to our control model. The hits included both novel miRNAs and miRNAs previously associated with ALS that potentially regulate several predicted genes and pathways that may be important for pathogenesis. Accordingly, these findings highlight specific miRNAs that may shed light on relevant disease pathways and could represent potential biomarkers and reversible treatment targets for ALS.

Keywords: amyotrophic lateral sclerosis, trans-activation response element DNA/RNA-binding protein of 43 kDa (TDP43), microRNAs, cytoplasmic aggregates, profiling

INTRODUCTION

Amyotrophic lateral sclerosis (ALS) is a neurodegenerative disease characterized by cortical, brainstem, and spinal cord motor neuron loss that results in progressive skeletal muscle weakness and atrophy (Brown and Al-Chalabi, 2017). There is currently no effective cure and most patients die within 3–5 years of diagnosis. The disease can occur as familial ALS (fALS), which constitutes around 15% of ALS incidence, or the more frequent sporadic ALS (sALS; Brown and Al-Chalabi, 2017; Chia et al., 2018; Goutman et al., 2018; Oskarsson et al., 2018).

The precise underlying etiology of ALS is not completely understood; however, a genetic cause has been identified in approximately 70% of fALS cases (Chia et al., 2018). The associated genetic changes (Brown and Al-Chalabi, 2017; Chia et al., 2018; Goutman et al., 2018) include expansions in C9orf72 (Balendra and Isaacs, 2018) and mutations in the RNA-binding proteins trans-activation response element DNA/RNA-binding protein of 43 kDa (TDP43; Sreedharan et al., 2008) and fused in sarcoma (FUS; Kwiatkowski et al., 2009; Vance et al., 2009). fALS and sALS share similarities in histopathological features, with over 90% of cases exhibiting TDP43 protein inclusions in the cytoplasm of the diseased brain and spinal cord neurons and glia (Hardiman et al., 2017). Moreover, aberrant protein and RNA metabolism and altered epigenetic mechanisms, such as those involving microRNAs (miRNAs), are recurrent themes among the dysregulated pathways (Vucic et al., 2014; Paez-Colasante et al., 2015; Brown and Al-Chalabi, 2017; Jimenez-Pacheco et al., 2017).

miRNAs are evolutionarily conserved ~22 nucleotide-long non-coding RNAs that post-transcriptionally regulate several mRNA targets, generally by binding to their 3' untranslated region, which marks them for translational repression and eventual degradation (Lagos-Quintana et al., 2001; Lau et al., 2001; Lee and Ambros, 2001). This regulation alters the gene expression profile and elicits changes downstream, thereby modulating physiological processes (Engels and Hutvagner, 2006; Selbach et al., 2008). miRNAs undergo a complex maturation process that includes the interaction of its primary (pri-miRNA) and precursor forms (pre-miRNA) with nuclear and cytoplasmic enzyme complexes and RNA binding proteins, including TDP43 (Kawahara and Mieda-Sato, 2012; Loffreda et al., 2015). miRNAs are highly expressed in the nervous system, and miRNA dysregulation occurs in multiple neurodegenerative diseases (Paez-Colasante et al., 2015; Tan et al., 2015; Maoz et al., 2017; Quinlan et al., 2017; Singh and Sen, 2017; Dolati et al., 2018), including ALS (Paez-Colasante et al., 2015; Rinchetti et al., 2018; Gagliardi et al., 2019). Of particular relevance, differentially expressed miRNAs have been detected in ALS patient spinal cord autopsy tissue, cerebrospinal fluid (CSF), and plasma, and are proposed as potential ALS biomarkers (Campos-Melo et al., 2013; Takahashi et al., 2015; Figueroa-Romero et al., 2016; Joilin et al., 2019). The driving force for miRNA dysregulation in ALS, however, has not been fully elucidated.

Complex molecular networks and dynamic cross-talk are likely involved in ALS-associated dysregulation (Jobe et al., 2012; Poddar et al., 2017), and TDP43, as an RNA binding

protein, may play an integral role (Birsa et al., 2020). Over 50 mutations to *TARDBP*, the gene encoding TDP43, occur in fALS (Kapeli et al., 2017). While TDP43 normally shuttles between the nucleus and cytoplasm (Chen-Plotkin et al., 2010; Bhardwaj et al., 2013; Gao et al., 2018), mutations and cellular stress skew the localization of mutant and/or wild-type (WT) TDP43 from the nucleus to the cytoplasm (Barmada et al., 2010), generating cytoplasmic TDP43 (cyTDP43) inclusions (Neumann et al., 2006; Zhang et al., 2008; Liu-Yesucevitz et al., 2010). WT or mutant TDP43 overexpression in motor neuron-like cells also interferes with miRNA biogenesis (Emde et al., 2015), and overexpressed mutant TDP43 promotes the formation of stress granules, which interact with and inhibit miRNA processing (Emde et al., 2015; Paez-Colasante et al., 2015; Weskamp and Barmada, 2018; Chen and Cohen, 2019). Additionally, TDP43 knockdown in neuroblastoma cells markedly affects miRNA levels (Kawahara and Mieda-Sato, 2012; Di Carlo et al., 2013), and TDP43 profoundly influences vital cellular processes through binding to several RNA targets in neurons (Sephton et al., 2011; Honda et al., 2013). Taken together, these findings are consistent with a role for TDP43 inclusions in RNA dysregulation during ALS and constitute a potential pathological mechanism that may lead to neuronal injury.

While suggestive of a causal relationship, however, our current understanding lacks insight into specific mechanisms whereby cyTDP43 inclusions may interfere with miRNA bioavailability and/or function. To address this gap in our knowledge, we used a high-throughput assessment of miRNA levels associated with multiple TDP43 pathological states to identify specific changes in miRNA/protein binding linked with cyTDP43. Our results expand the understanding of how TDP43 mislocalization affects specific miRNA levels in ALS, and thereby provide a foundation to ultimately gain new mechanistic insights and uncover untapped diagnostic and therapeutic avenues in ALS.

MATERIALS AND METHODS

TDP43-miRNA Binding Assays

We used a native gel mobility shift assay (Ramsey and Kelm, 2009; Poddar et al., 2017) to assess the formation of TDP43-miRNA complexes for three miRNAs known to associate with TDP43: miR-132, miR-143, and miR-574-5p (Buratti et al., 2010; Kawahara and Mieda-Sato, 2012; Freischmidt et al., 2013). The select miRNAs were purchased from Integrated DNA Technologies (Coralville, IA, USA), 5'-end-labeled with ³²P using T4 polynucleotide kinase (PNK; New England Biolabs, Ipswich, MA, USA), and excess unincorporated isotope was removed with a Centri-Spin 10 column (Invitrogen, Thermo Fisher Scientific, Carlsbad, CA, USA). Binding affinity was measured by mixing the 5'-³²P-end labeled miRNAs with excess denatured full-length TDP43 (0.05, 0.125, 0.25, 0.5, or 1.25 μM; cat# ab156345, Abcam, San Francisco, CA, USA) for 30 min at room temperature in buffer [14 mM Tris (pH 8.0), 35 mM KCl, 14 mM NaCl, 1.4 mM MgCl₂, 14% glycerol, 0.7 mM dithiothreitol (DTT)]. Samples were then electrophoresed for 3 h at 4°C on a native 0.5× Tris-borate-EDTA (TBE) gel (19:1 crosslink). Bands were visualized

by exposure to a storage PhosphorImager screen for 30 min and scanned by a Typhoon PhosphorImager (GE Healthcare, Chicago, IL, USA).

Apparent binding affinities of TDP43 to select miRNAs of varying UG repeats (bolded and underlined below) were next measured *via* a direct colorimetric enzyme-linked immunosorbent assay (ELISA; Rumora et al., 2010, 2013). Briefly, 3'-biotinylated miRNAs (miR-574-5p, 5'-UGAGUGUGUGUGUGAGUGUGU-3'; miR-652-3p, 5'-AAUGGCCACCUAGGGUUGUG-3'; and miR-204-5p, 5'-UCCCCUUUGUCAUCCUAUGCCU-3') were synthesized by Integrated DNA Technologies. Serial dilutions of each 3'-biotinylated miRNA were immobilized on a 96-well StreptaWell microplate (Roche Applied Science, Penzberg, Germany) at concentrations ranging from 0 to 20 nM for miR-574, 0–85 nM for miR-652, and 0–80 nM for miR-204 for 2 h at room temperature. Different concentration ranges were used for each 3'-biotinylated miRNA to achieve the saturable binding of TDP43 to individual miRNAs. Microplate wells were blocked with 2% ELISA grade BSA for 1 h at room temperature, and wells were washed after each step with wash buffer (20 mM HEPES pH 7.5, 150 mM NaCl, 1.5 mM MgCl₂, 0.05% v/v Tween 20). For TDP43 binding to immobilized miRNAs, pure full length TDP43 protein (5 nM; cat# ab224788, Abcam) was incubated for 12 h overnight at 4°C in binding buffer (wash buffer supplemented with 0.5 mM DTT, 1.0 µg/ml of an AC/TG nonspecific oligonucleotide, 0.2% w/v ELISA grade BSA). After the 12 h incubation, immobilized miRNA-protein complexes were detected with purified anti-TDP43 mouse monoclonal antibody (1.0 µg/ml; R&D, Minneapolis, MN) in antibody buffer (wash buffer supplemented with 0.2% w/v ELISA grade BSA) for 1 h at room temperature. A 1:8,000 dilution of secondary horseradish peroxidase (HRP)-coupled goat anti-mouse antibody (Santa Cruz Biotechnology, Dallas, TX, USA) was then incubated for 1 h at room temperature. Finally, 100 µl of ABTS chromogenic substrate solution (Millipore, Burlington, MA, USA) was added to each well and incubated for 1 h. Colorimetric measurements were taken at A405 every 30 min until saturation (maximum A₄₀₅ ~1) on a Synergy HTX multimode plate reader (BioTek, Winooski, VT, USA) equipped with Gen5 software (version 3.03). The EC₅₀ values for each TDP43-miRNA apparent affinity were determined by fitting the datasets to a four-parameter variable slope equation in Prism 6 (GraphPad, San Diego, CA, USA).

Plasmids

To generate stable doxycycline-inducible cell lines expressing eGFP-His-tagged TDP43 variants that primarily localized to the nucleus or cytoplasm, we first amplified eGFP-His from pGW1-T202-TDP43-eGFP-His (Barmada et al., 2010) using the primers 5'-ATA AGA ATG CGG CCG CAA CTA GAG CTG TTT GGG ACG-3' and 5'-CGG ACG CGT TTT TAG TGA TGG TGA TGG TGA TG-3'. The eGFP-His fragment was subcloned directionally into the NotI-MluI restriction sites (underlined in bold in the primer sequence) of the doxycycline-inducible pLVX-TRE3G lentiviral vector (Clontech, Takara Bio USA, Mountain View, CA, USA) to generate the pLVX-TRE3G-eGFP-His construct.

WT TDP43 from pGW1-TDP43WT-eGFP (Barmada et al., 2014) was next amplified using the primers 5'-CGG GAT CCA TGT CTG AAT ATA TTC GGG TAA CCG-3' and 5'-ATA GTT TAG CGG CCG CCA TTC CCC AGC CAG AAG A-3', and the WT TDP43 fragment was ligated directionally into the BamHI-NotI restriction sites (underlined in bold in the primer sequence) of the pLVX-TRE3G-eGFP-His construct to create the final pLVX-TRE3G-WT-TDP43-eGFP-His plasmid. PCR reactions were performed with Q5 High-Fidelity DNA Polymerase (New England BioLabs) and transformations with Stellar competent cells (Clontech, Takara Bio USA Mountain View, CA, USA), both according to the manufacturer's instructions. Missense mutations disrupting the two nuclear localization signals (Δ NLS) in TDP43 to force cytoplasmic localization were next introduced into the pLVX-TRE3G-TDP43WT-eGFP-His plasmid using site-directed mutagenesis as previously described (Winton et al., 2008; Barmada et al., 2010) to generate pLVX-TRE3G- Δ NLS-TDP43-eGFP-His. All sequences were verified by the University of Michigan Sequencing Core¹.

Generation of Doxycycline-Inducible Stable HeLa Cell Lines

HeLa cells were grown in Dulbecco's modified Eagle's medium (DMEM; 11965-092, Gibco, Thermo Fisher Scientific, Gaithersburg, MD, USA) supplemented with 10% fetal bovine serum (A3160401, Thermo Fisher Scientific, Gaithersburg, MD, USA) at 37°C in 10% CO₂. Confluent cells were transiently transfected with 100 ng of the pLVX-TRE3G-eGFP-His, pLVX-TRE3G-WT-TDP43-eGFP-His, or pLVX-TRE3G- Δ NLS-TDP43-eGFP-His constructs along with pLVX-EF1 α -Tet3G (Clontech, Takara Bio USA) using Lipofectamine 2000 reagent (Invitrogen) according to the manufacturer's protocol. Following a 6 h incubation, wells were rinsed and replenished with growth media containing the selection antibiotics puromycin (1 µg/ml; #P8833, Sigma, St. Louis, MO, USA) and geneticin (1 µg/ml; G418; #10131-035, Gibco) for 48 h. Doxycycline (1 µg/ml; #PHR1145, Sigma) was then added to the media to induce protein expression and confirm transfection. Transfection efficiency was determined to be about 20%, and stable lines were generated using a serial dilution protocol in 96-well plates (Corning Inc., Corning, NY, USA; Ryan, 2008). HeLa cells were monitored daily and scored for wells that contained a single colony, which was grown to confluence. Induction with doxycycline was performed to select eGFP-positive clones for expansion. A confluent sample from each expanded eGFP-expressing clone was fixed with 4% paraformaldehyde and stained with Hoechst reagent to visualize the nuclei and localize eGFP (*i.e.*, nuclear vs. cytoplasmic). Multiple clones were generated that varied modestly in the level of WT-TDP43-eGFP-His, Δ NLS-TDP43-eGFP-His, or eGFP-His expression, and those with the most optimal eGFP level (high expression with normal cellular morphology and survival) were selected for further experiments.

¹<https://brcf.medicine.umich.edu/cores/advanced-genomics/>

Subcellular Fractionation

Fractionation was used to examine the subcellular localization of TDP43 variant expression (Barmada et al., 2010; Archbold et al., 2018). Briefly, WT-TDP43-eGFP-His-, Δ NLS-TDP43-eGFP-His-, or eGFP-His-expressing HeLa cells were plated at a density of 1×10^5 cells/well, incubated for 48 h, and then half of the plates were induced with 1 μ g/ml doxycycline for an additional 48 h. To efficiently capture cyTDP43-bound miRNAs, the stable cell lines were irradiated in a UVP HL-2000 HybriLinker UV cross-linker oven (Thermo Fisher Scientific) at 400 mJ/cm² and again at 200 mJ/cm² (King et al., 2014), and then cells were protected from light, detached by scraping in the buffer, and harvested by centrifugation (4 min, 1,000 rpm, 4°C). Cells were lysed as previously reported (Sharma et al., 2011; King et al., 2014) on ice for 5 min in resuspension buffer [RSB: 10 mM Tris (pH 7.4), 10 mM NaCl, 3 mM MgCl₂, Complete Protease Inhibitor Cocktail (Roche), 0.2 U/ μ l RNase Inhibitor (cat# N8080119, Applied Biosystems, Thermo Fisher Scientific, Foster City, CA, USA), and DNase per the manufacturer's instructions (cat# 1023460, Qiagen, Hilden, Germany)]. RSB supplemented with 0.6% IGEPAL (#CA-630, Sigma) was added to the lysate and incubated for 5 min before centrifugation (15 min, 2000 G, 4°C) to separate the cytosolic (supernatant) and nuclear (pellet) fractions. Imidazole (10 mM; #10250-25g, Sigma) was added to the cytoplasmic supernatant fraction. The nuclear pellet fraction was resuspended in RSB, centrifuged (10 min, 2000 G, 4°C), and then the resulting nuclear pellet was resuspended and sonicated in CHAPS lysis buffer (5 M NaCl, 1 M imidazole, 0.5 M Na₂PO₄, 1 M NaH₂PO₄, and 10% CHAPS, pH 8.0), incubated on ice for 30 min, and centrifuged (15 min, 6800 G, 4°C; Figueroa-Romero et al., 2009). An aliquot was removed at each step and total protein was measured using a Pierce BCA Protein Assay Kit (cat# 23227, Thermo Fisher Scientific) following the manufacturer's instructions before mixing with 2 \times sample buffer [100 mM Tris (pH 6.8), 4% SDS, 10% glycerol, 0.015% bromophenol blue; Figueroa-Romero et al., 2009]. To validate the subcellular fractionation efficiency, samples were boiled for 5 min in 2 \times sample buffer and subjected to Western blot analysis.

WT-TDP43-eGFP-His and Δ NLS-TDP43-eGFP-His Pull-Down

To further evaluate TDP43 variant expression patterns, WT-TDP43-eGFP-His, Δ NLS-TDP43-eGFP-His, and control eGFP-His were pulled down *via* their His tags from the subcellular fractions using nickel-agarose (Ni²⁺) beads (Qiagen; Figueroa-Romero et al., 2009). Briefly, 40 μ l Ni²⁺-beads prewashed in CHAPS buffer were added to each 600 μ l sample and rotated overnight at 4°C. Beads were then washed three times with CHAPS buffer and divided into two aliquots, one for protein and one for RNA extraction. A bead-only sample was included throughout the rest of the protocol as a negative control.

For protein extraction, bead aliquots were washed twice with CHAPS glycanase buffer (50 mM NaCl, 45 mM Na₂HPO₄, 5 mM NaH₂PO₄, 0.1% CHAPS, pH 8.0) and centrifuged between washes (15 s, max speed). Protein concentration was measured

using a Pierce BCA Protein Assay Kit (cat# 23227, Thermo Fisher Scientific) following the manufacturer's instructions, and the subcellular fractions were resuspended in 3 \times EDTA sample buffer (150 mM Tris (pH 6.8), 10 mM EDTA, 6% SDS, 15% glycerol, 0.0225% bromophenol blue) supplemented with 20 mM β -mercaptoethanol. Samples were incubated at 50°C for 20 min before Western blot analysis (Figueroa-Romero et al., 2009; King et al., 2014).

For extracting miRNAs, bead aliquots from the cytoplasmic fractions were washed twice with 1 \times PXL (0.1% SDS, 0.5% Triton X-100, 0.5% deoxycholate in 1 \times PBS) and twice with 5 \times PXL. Samples were then boiled for 3 min to reverse cross-linking (King et al., 2014), and QIAzol (Qiagen) was added and samples were stored at -80°C. Next, a miRNeasy Mini Kit (cat# 217004, Qiagen) was used to extract total RNA, enriched in cyTDP43-bound miRNAs. Purified RNA was treated with RNase-free DNase and stored at -80°C until required for cDNA synthesis or miRNA profiling.

Western Blot

A 15 μ g aliquot of protein per sample was resolved on a denaturing 10% polyacrylamide gel, and proteins were transferred to polyvinylidene difluoride (PVDF) membranes using a semidry blotter by established standard protocols (Figueroa-Romero et al., 2009; Lunn et al., 2009). Blots were probed overnight at 4°C with the following primary antibodies: rabbit anti-TDP43 (1:1,000; cat#A260, Cell Signaling Technology, Danvers, MA, USA), rabbit anti-histone 2B (H2B) member S (1:500; cat# NB100-56347, Novus Biologicals, Littleton, CO, USA), rabbit anti-GFP (1:1,000; cat#2555, Cell Signaling Technology), and rat anti- α -tubulin (1:5,000; cat#ab6160, Abcam). The next day, blots were rinsed and probed for 50 min at room temperature with appropriate HRP-conjugated secondary antibodies (1:1,000; Santa Cruz Biotechnology or New England Biolabs), then rinsed and visualized by enhanced chemiluminescence with Prime Western Blotting Detection Reagent (Amersham, GE Healthcare, Chicago, IL, USA).

miRNA NanoString Profiling, Analysis, and Validation

To evaluate miRNA profiles associated with cyTDP43, total RNA from the cytoplasmic fractions pulled-down with Ni²⁺-beads for WT-TDP43-eGFP-His, Δ NLS-TDP43-eGFP-His, and eGFP-His lines ($n = 4$ for each line) was processed using the nCounter Human v3A miRNA Gene List (NanoString Technologies, Seattle, WA, USA) as published previously (Wohlfarth et al., 2017). A nCounter Digital Analyzer counted individual fluorescent barcodes that quantified and identified levels of up to 800 human-specific target miRNA molecules. nSolver Analysis Software 3.0 (NanoString Technologies) was used to background subtract and normalize the top 100 miRNA counts. Fold-change differences for WT-TDP43- or Δ NLS-TDP43-associated miRNAs relative to control (eGFP-His) were identified using $P < 0.05$ as the significance cutoff. Significant

miRNAs were then analyzed using mirPath v.3² (Vlachos et al., 2015) using a false discovery rate corrected *P*-value threshold of 0.05 and a microT threshold of 0.8 for predicted miRNA targets in the microT-CDS database to identify Kyoto Encyclopedia of Genes and Genomes (KEGG) pathways³ that associate with the cyTDP43-interacting miRNAs.

To validate the NanoString dataset, quantitative real-time PCR (qPCR) of select cyTDP43-associated miRNAs was performed using TaqMan Universal PCR Master Mix, TaqMan MicroRNA Assays (Thermo Fisher Scientific), and a 1:100 dilution of the pre-amplified NanoString analysis template as previously described (Figueroa-Romero et al., 2016) using the standard TaqMan protocol on a StepOnePlus Real-Time PCR System (Applied Biosystems). The cycle threshold (CT) values representing miRNA expression in the samples were calculated using StepOnePlus software and normalized to miR-92a-3p, a miRNA with a low coefficient of variation across samples. Next, Δ CT and $\Delta\Delta$ CT were calculated relative to the control group. miRNA levels were expressed as the mean \pm standard error of the mean (SEM) for triplicates and statistically significant differences between either WT-TDP43-eGFP-His or Δ NLS-TDP43-eGFP-His to control (eGFP-His) were evaluated with a two-sample equal-variance Student's *t*-test (Prism 5, GraphPad, San Diego, CA, USA); *P* < 0.05 was considered statistically significant.

RESULTS

TDP43 Binds Differentially to Distinct miRNAs

To gain insight into TDP43's ability to interact with specific miRNAs, we first used a native gel mobility shift assay to evaluate binding of denatured TDP43 to miR-132, miR-143, and miR-574, miRNAs all previously reported to associate with TDP43 (Buratti et al., 2010; Kawahara and Mieda-Sato, 2012; Freischmidt et al., 2013). Results demonstrated a band shift only for miR-574 (Figure 1A), with no observable shift for miR-132 or miR-143, suggesting that denatured TDP43 has a strong affinity only for miR-574. Since TDP43 binding often relies on associations with UG repeats (Ayala et al., 2005; Bhardwaj et al., 2013), the apparent binding affinity of TDP43 for miR-574 (9 UG repeats), miR-652 (3 UG repeats), and miR-204 (2 UG repeats) was next evaluated using a colorimetric ELISA to detect natively folded TDP43 bound to surface-captured biotinylated miRNAs (Rumora et al., 2010, 2013). EC50 values were determined for the binding of TDP43 to each miRNA from a titration of the biotinylated miRNAs. TDP43 had the highest apparent affinity for miR-574 (EC50 = 2.84 nM), a slightly lower binding affinity for miR-652 (EC50 = 6.41 nM), and the lowest binding affinity for miR-204 (EC50 = 37.7 nM; Figure 1B). These EC50s are proportional to the number of UG repeats in each miRNA sequence (miR-574 > miR-652 > miR-204) and support the contention that UG content dictates the relative binding affinity of TDP43 (Bhardwaj et al., 2013).

²<http://snf-515788.vm.okeanos.grnet.gr/>

³<http://www.genome.jp/kegg/>

Cells Expressing WT-TDP43-eGFP-His and Δ NLS-TDP43-eGFP-His Reflect Differential Subcellular TDP43 Localization

To provide a model to study the effect of altered TDP43 cellular localization on miRNAs, we established doxycycline-inducible HeLa cell lines that stably express eGFP- and His-tagged WT-TDP43 or Δ NLS-TDP43, along with eGFP-His-expressing controls. Upon doxycycline-induced expression, eGFP imaging revealed primarily nuclear localization of overexpressed WT-TDP43-eGFP-His vs. primarily cytoplasmic localization of Δ NLS-TDP43-eGFP-His (Figure 2A). This differential localization was further supported by Western blotting of eGFP in nuclear and cytoplasmic fractions. α -Tubulin, a cytoplasmic protein, was detected in whole-cell lysates and cytoplasmic fractions for all three cell lines, as expected (Figure 2B, top panel). The nuclear marker H2B was present in whole-cell lysates and nuclear fractions of all three cell lines, and only weakly detected in their cytoplasmic fractions (Figure 2B, middle panel). eGFP expression was also confirmed in whole-cell lysates of all three cell lines (Figure 2B, bottom panel), although the expression levels were low in some fractions, so we enriched using a Ni²⁺-bead pull-down assay for His-tagged proteins to better evaluate subcellular localization in each fraction. The resulting data corroborated the primarily cytoplasmic localization of Δ NLS-TDP43-eGFP-His (Figure 2C) and verified the largely nuclear localization of WT-TDP43-eGFP-His that was accompanied by some anticipated cytoplasmic localization from its natural nucleus-cytoplasm shuttling role (Li et al., 2015; Weskamp and Barmada, 2018; Figure 2C). Of note, the lower of the two TDP43 bands in the nuclear fractions likely reflects endogenous TDP43 associating with the eGFP-His-tagged TDP43 aggregates, whereas the higher band represents the eGFP-His fusion protein. The third band in the Δ NLS-TDP43-eGFP-His cytoplasmic fraction most likely reflects a proteolytic TDP43 cleavage product (Li et al., 2015; Weskamp et al., 2020). Together, these data support our ability to efficiently separate the cytoplasmic and nuclear compartments for all three cell lines, with minimal inter-fraction contamination, and our ability to effectively pull down TDP43 *via* its His tag.

WT-TDP43-eGFP-His- and Δ NLS-TDP43-eGFP-His-Expressing Cells Exhibit Differential miRNA Profiles

To identify miRNAs that interact with cytoplasmic WT-TDP43-eGFP-His or Δ NLS-TDP43-eGFP-His, we performed NanoString miRNA profiling of TDP43-bound miRNAs isolated by Ni²⁺-pull-down from cytoplasmic fractions of the respective stable HeLa cell lines. Appreciable target detection occurred for most miRNAs across all samples, and assessment of fold-changes vs. the control eGFP-His line identified 65 significantly altered cyTDP43-associated miRNAs (Figure 3 and Table 1). For WT-TDP43-eGFP-His cells, 11 miRNAs decreased and 14 increased in level (Figure 3B). In the Δ NLS-TDP43-eGFP-His cell line with primarily cytoplasmic TDP43 localization, more miRNAs satisfied the criteria for significant fold-enrichment, with 29 decreased and 23 increased in levels (Figure 3C).

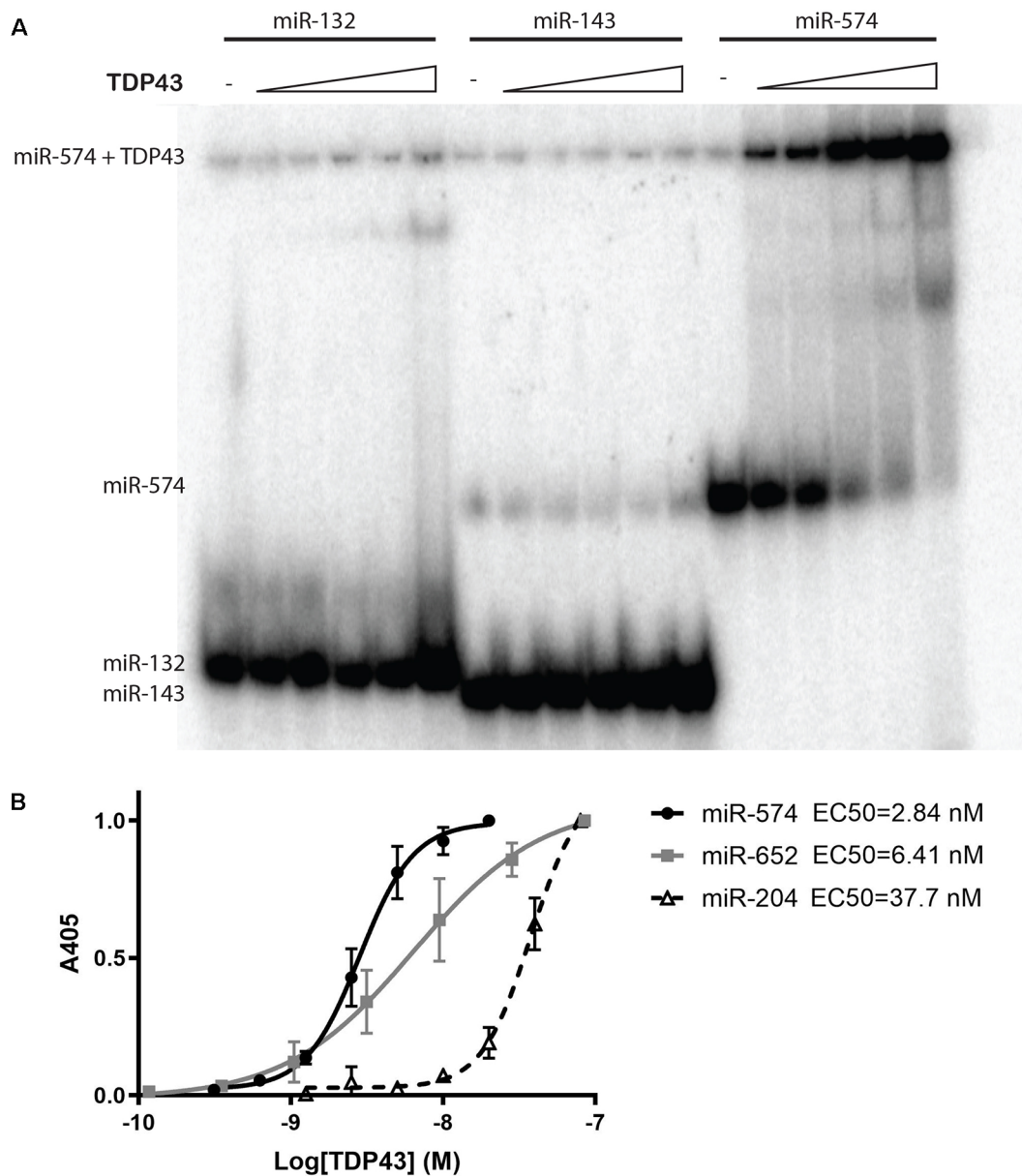


FIGURE 1 | Trans-activation response element DNA/RNA-binding protein of 43 kDa (TDP43) binding specificity and apparent binding affinities for select microRNAs (miRNAs). **(A)** A native gel mobility shift assay was used to evaluate the association between TDP43 and previously associated miRNAs: miR-132, miR-143, and miR-574. Trace amounts of ^{32}P -radiolabeled RNA (5 nM) were incubated with increasing concentrations of TDP43 (0, 0.05, 0.125, 0.25, 0.5, and 1.25 mM) and analyzed on a 12.5% native PAGE gel. A shift in band size was observed only for miR-574 (right). **(B)** Apparent binding affinities (EC₅₀s) of TDP43 for select miRNAs with varying numbers of UG repeats were determined using a titration of biotinylated miRNAs in a colorimetric ELISA. EC₅₀s are proportional to the number of UG repeats in each miRNA (miR-574, nine repeats > miR-652, three repeats > miR-204, two repeats).

Interestingly, nine miRNAs (four decreased and five increased) in the WT-TDP43-eGFP-His cells and 11 miRNAs (six decreased and five increased) in the ΔNLS -TDP43-eGFP-His cells were enriched by more than 3-fold. Moreover, 12 miRNAs were present in both cell lines and exhibited similar over- or under-enrichment.

To validate the NanoString profiling results, we performed qPCR on the same samples used for miRNA profiling

for miR-204-5p and miR-129-5p. qPCR miRNA levels were normalized to miR-92a, which has a low coefficient of variation relative to other miRNAs in all cell lines (data not shown). Similar to the NanoString data, qPCR showed statistically significant increases in miR-204-5p and levels in both WT-TDP43-eGFP-His and ΔNLS -TDP43-eGFP-His HeLa cell lines (**Figures 4A,C**). Likewise, miR-129-5p increased in both WT-TDP43-eGFP-His and

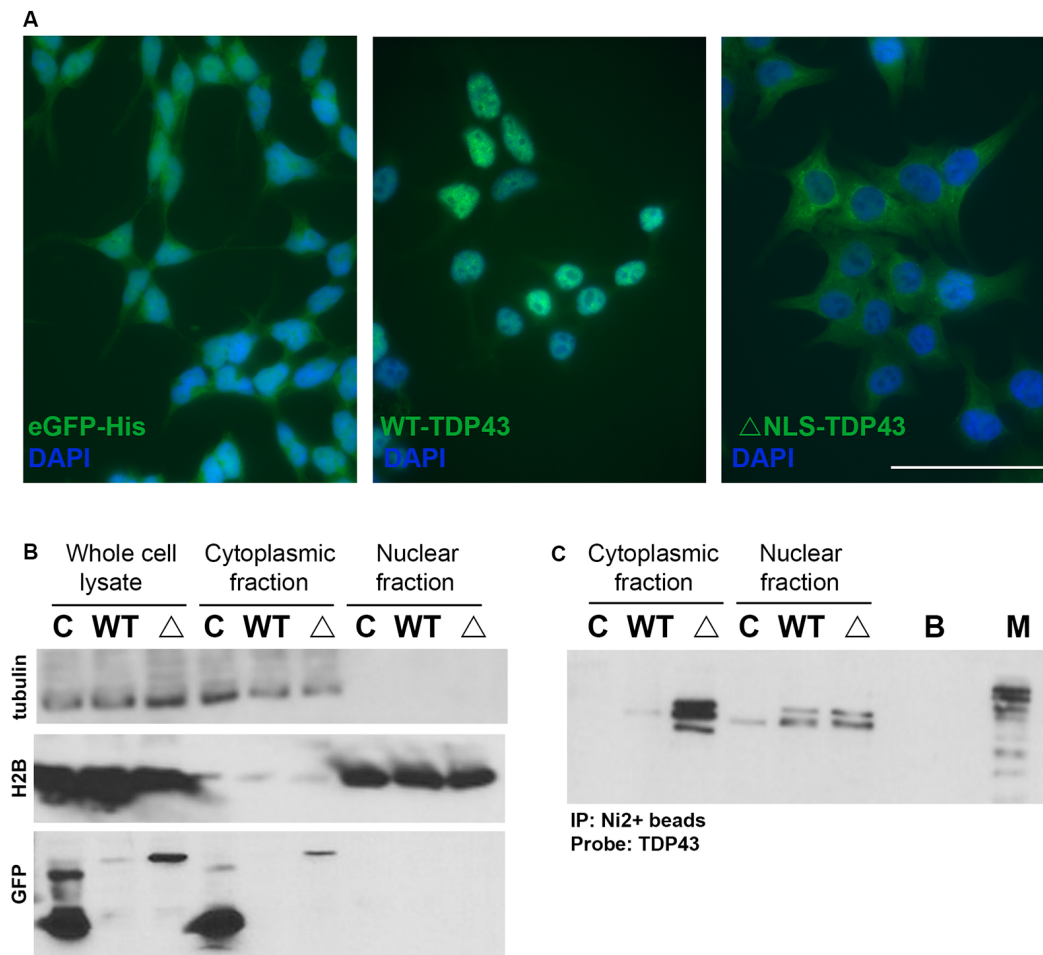


FIGURE 2 | Doxycycline-inducible stable cell lines expressing TDP43 variants. **(A)** Representative images of control (eGFP-His), wild-type (WT)-TDP43-eGFP-His (WT-TDP43), and Δ NLS-TDP43-eGFP-His (Δ NLS-TDP43) stable HeLa cell lines depict primarily nuclear expression for WT-TDP43 and predominantly cytoplasmic expression for Δ NLS-TDP43. Scale bar = 50 μ m. **(B)** Immunoblotting of whole-cell lysates and cytoplasmic and nuclear fractions for α -tubulin (cytoplasmic marker; top panel), H2B (nuclear marker; middle panel), and eGFP (a marker for expression of the eGFP-His-tagged doxycycline-inducible plasmids) following subcellular fractionation of the control (C), WT-TDP43-eGFP-His (WT), and Δ NLS-TDP43-eGFP-His (Δ) lines. eGFP immunoblotting demonstrates that eGFP-His (lower band) is expressed in the whole-cell lysates and cytoplasmic fraction of the control cell line, while eGFP-His-tagged TDP43 (upper band) is present in the whole-cell lysates and cytoplasmic fraction of the WT-TDP43-eGFP-His and Δ NLS-TDP43-eGFP-His cell lines, although only marginal expression seen in the WT-TDP43-eGFP-His cell line. **(C)** TDP43 immunoblotting following pull-down of the His-tagged proteins using Ni²⁺ beads. Δ NLS-TDP43-eGFP-His is detected mainly in the cytoplasmic fraction, with some expression also seen in the nuclear fraction, while WT-TDP43-eGFP-His is more highly abundant in the nuclear fraction, though modest expression is also seen in the cytoplasmic fraction. The slightly higher bands in both TDP43 lines represent the TDP43-eGFP-His fusion proteins, while the lower bands represent endogenous TDP43. In the cytoplasmic fraction, Δ NLS-TDP43-eGFP-His also exhibits a third band (lowest) that likely reflects a proteolytic cleavage product of TDP43. C = eGFP-His; WT = WT-TDP43-eGFP-His; Δ = Δ NLS-TDP43-eGFP-His; B = Ni²⁺ bead only control; M = marker/ladder.

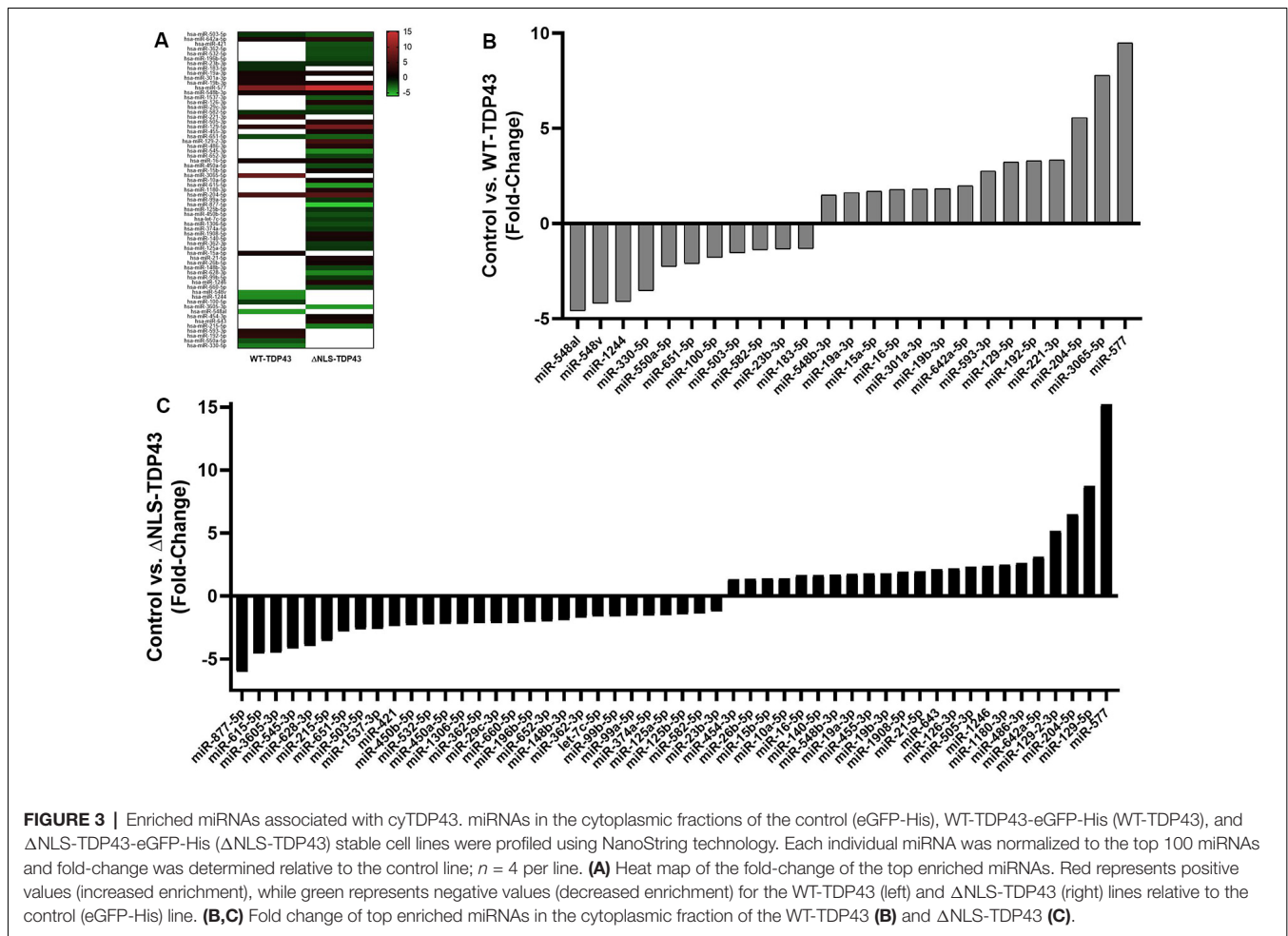
Δ NLS-TDP43-eGFP-His cell lines but did not reach statistical significance (Figures 4B,C).

miRNA pathway analysis of the 65 miRNAs using mirPath v.3 (Vlachos et al., 2015) further revealed several predicted gene targets and associated KEGG pathways that offered insight into the relevance of the identified cyTDP43-interacting miRNAs. Pathways represented in both WT-TDP43-eGFP-His and Δ NLS-TDP43-eGFP-His included multiple cancer and neuronal function and health pathways, such as GABAergic and glutamatergic synapses, axon guidance, and neurotrophin signaling pathways (Figure 5; Supplementary Tables S1, S2).

Taken together, these data indicate that TDP43 expression and localization significantly affects the levels of multiple miRNAs, which are predicted to affect several genes and biological pathways that are relevant to nervous system health and disease.

DISCUSSION

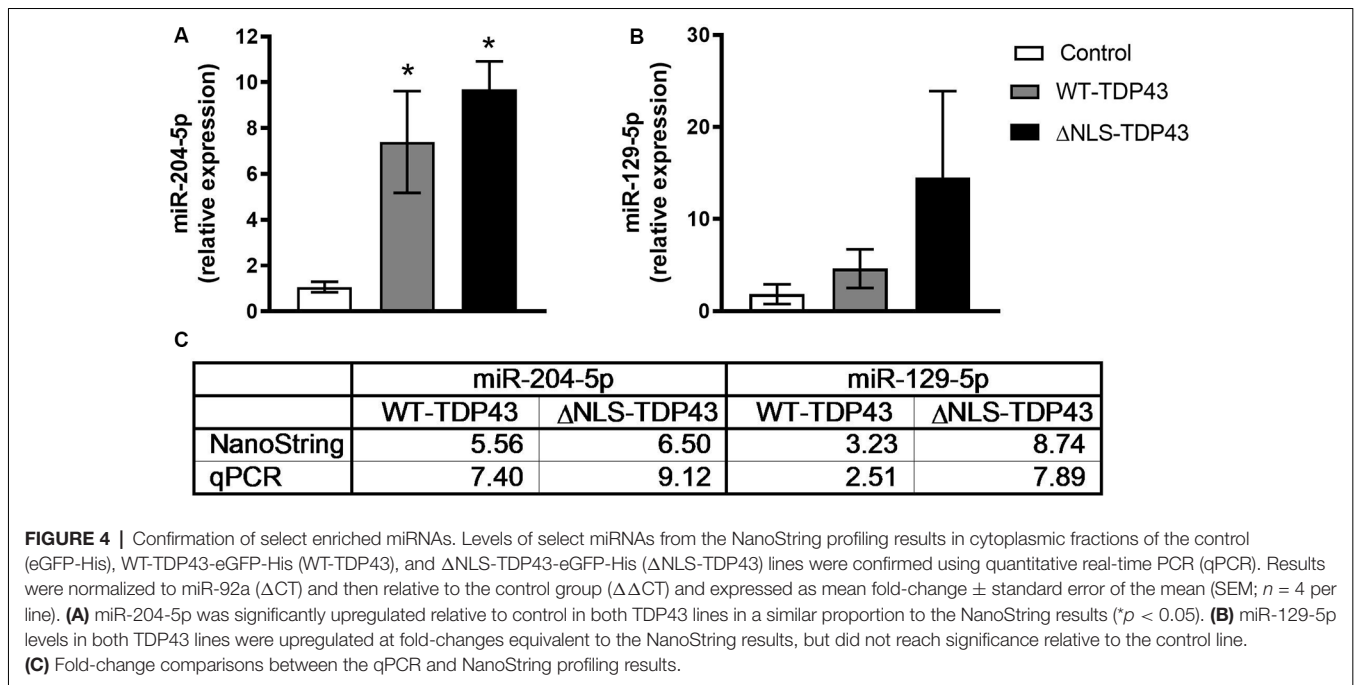
TDP43 mutations are linked to ALS (Kapeli et al., 2017), and cyTDP43 is a universal histopathological hallmark of *postmortem* brain and spinal cord tissue from fALS and sALS subjects



(Neumann et al., 2006; Zhang et al., 2008; Liu-Yesucevitz et al., 2010). However, the implications of these cytoplasmic inclusions on key cellular processes, including gene expression, have not been fully elucidated. TDP43 is central to miRNA biogenesis, and its ability to directly interact with miRNAs regulates expression of numerous genes (Kawahara and Mieda-Sato, 2012; King et al., 2014; Emde et al., 2015; Loffreda et al., 2015; Paez-Colasante et al., 2015). We hypothesized that one consequence of TDP43 cytoplasmic translocation is aberrant protein/miRNA interactions that may ultimately affect cell function and viability through epigenetic mechanisms. To address this idea, we first showed that TDP43 exhibits differential binding affinity for specific miRNAs and that binding affinities correlate with the number of miRNA UG repeats. This suggests that cyTDP43 may preferentially affect certain miRNAs during disease pathogenesis. Next, using stable cell lines expressing inducible TDP43 variants with primarily nuclear (WT-TDP43-eGFP-His) or cytoplasmic (Δ NLS-TDP43-eGFP-His) subcellular localization, we identified 65 differentially enriched miRNAs that associate with cyTDP43, including known and novel hits that potentially regulate multiple predicted genes and pathways. Together, these findings provide insight into the

consequences of TDP43 mislocalization in ALS by identifying specific miRNAs that associate with cyTDP43. These data could ultimately shed light on pathogenic mechanisms, biomarkers, and reversible ALS treatment targets.

TDP43 is normally predominantly found in the nucleus; however, ALS-associated mutations and/or cellular stress can prompt hyper-phosphorylation and sequestration into insoluble, ubiquitin-positive, denatured cytoplasmic aggregates (Neumann et al., 2006, 2009). Previous studies also indicate that TDP43 knockdown is toxic (Sephton et al., 2010; Iguchi et al., 2013; Barmada et al., 2015), that TDP43 toxicity more closely correlates with increased cyTDP43 than with the level of nuclear TDP43 (Barmada et al., 2010), and that cyTDP43 clearance can exert beneficial effects on neuronal survival (Barmada et al., 2014) and functional outcomes (Walker et al., 2015). cyTDP43 has thus been the focus of multiple *in vitro* and *in vivo* studies in recent years (Miguel et al., 2011; Walker et al., 2015; Birsá et al., 2020). Of particular relevance is the rNLS8 ALS mouse that exhibits inducible expression of Δ NLS-TDP43 in motor neurons. This transgenic mouse recapitulates many of the pathologic characteristics of ALS, including cyTDP43 aggregation, motor neuron



death, increases in CSF neurofilament levels, neuromuscular junction loss, muscle atrophy, and abnormal compound muscle axon potentials measured by electromyogram (Spiller et al., 2016a,b, 2018, 2019). However, a complete understanding of the effect TDP43 mislocalization has on specific miRNAs is lacking. This is important for neuronal health because cytoplasmic TDP43 aggregates can interact with and sequester key miRNAs, thus limiting their ability to perform their normal regulatory functions. Cytoplasmic TDP43 aggregates also impair normal miRNA maturation through a loss of nuclear localization and interactions with miRNA biosynthetic pathway components (Barmada and Finkbeiner, 2010; Kawahara and Mieda-Sato, 2012; Weskamp and Barmada, 2018). Herein, we specifically focused on understanding how cytoplasmic translocation of TDP43 affects miRNA dynamics as another potential pathomechanism.

Before examining the impact of cyTDP43 on miRNAs, we first assessed TDP43 interactions and binding affinities to three specific miRNAs known to associate with TDP43: miR-132, miR-143, and miR-574-5p (Buratti et al., 2010; Kawahara and Mieda-Sato, 2012; Freischmidt et al., 2013). We found that denatured TDP43 complexed with miR-574-5p, a miRNA first predicted to bind to TDP43 based on its UG-repeat regions in primary sequence (Buratti et al., 2010), but not miR-132 or miR-143, within the detection limit of our native gel mobility shift assay. We further verified that apparent binding affinities of TDP43 to miRNAs increased relative to the number of UG repeats; miR-574-5p with nine UG repeats had the highest affinity relative to miRNAs with only two or three UG repeats. Though all three miRNAs we selected to examine are known to exhibit altered levels in CSF and serum from ALS subjects (Freischmidt et al., 2013), we did

not observe interactions between TDP43 and miR-132 or miR-143. This may be related to the use of denatured TDP43 in our assay, selected because of its biological representation of TDP43 aggregates, or due to differential regulation of the miRNAs in the CSF and serum vs. cells, suggesting that cell-type-specific mechanisms may be involved (Freischmidt et al., 2013). Alternatively, TDP43 can bind UG-rich sequences as well as other secondary structures in pri- and pre-miRNAs (Kawahara and Mieda-Sato, 2012). Nonetheless, our data support the idea that TDP43 localization can differentially affect specific miRNAs.

To better understand the role of TDP43 mislocalization on miRNA dynamics, we created stable inducible cell lines that express predominantly nuclear (WT) or cytoplasmic (Δ NLS) TDP43 variants in HeLa cells, which are a known and reliable model of TDP43 pathology (Ayala et al., 2008; Ling et al., 2010; Gu et al., 2017). cyTDP43 expression was regulated by a doxycycline-inducible promoter to prevent cytotoxicity from the overexpressed or mutant proteins (Walker et al., 2015), a GFP tag facilitated visualization, and a His-tag was present to leverage cyTDP43/miRNA profiling using a pulldown assay. We confirmed moderate WT-TDP43 overexpression that led to primarily nuclear expression and marginal cytoplasmic expression, similar to other WT-TDP43 overexpression models (Neumann et al., 2006, 2009; Barmada et al., 2015; Li et al., 2015; Wang et al., 2015). We similarly verified that the mutant Δ NLS-TDP43 was localized to the cytoplasm, leading to diffuse or aggregated cyTDP43 as in previous *in vitro* cell models (Winton et al., 2008; Barmada et al., 2010; Liu-Yesucevitz et al., 2010), *in vivo* animal models (Wils et al., 2010; Miguel et al., 2011; Walker et al., 2015), and human *postmortem* neuronal tissue

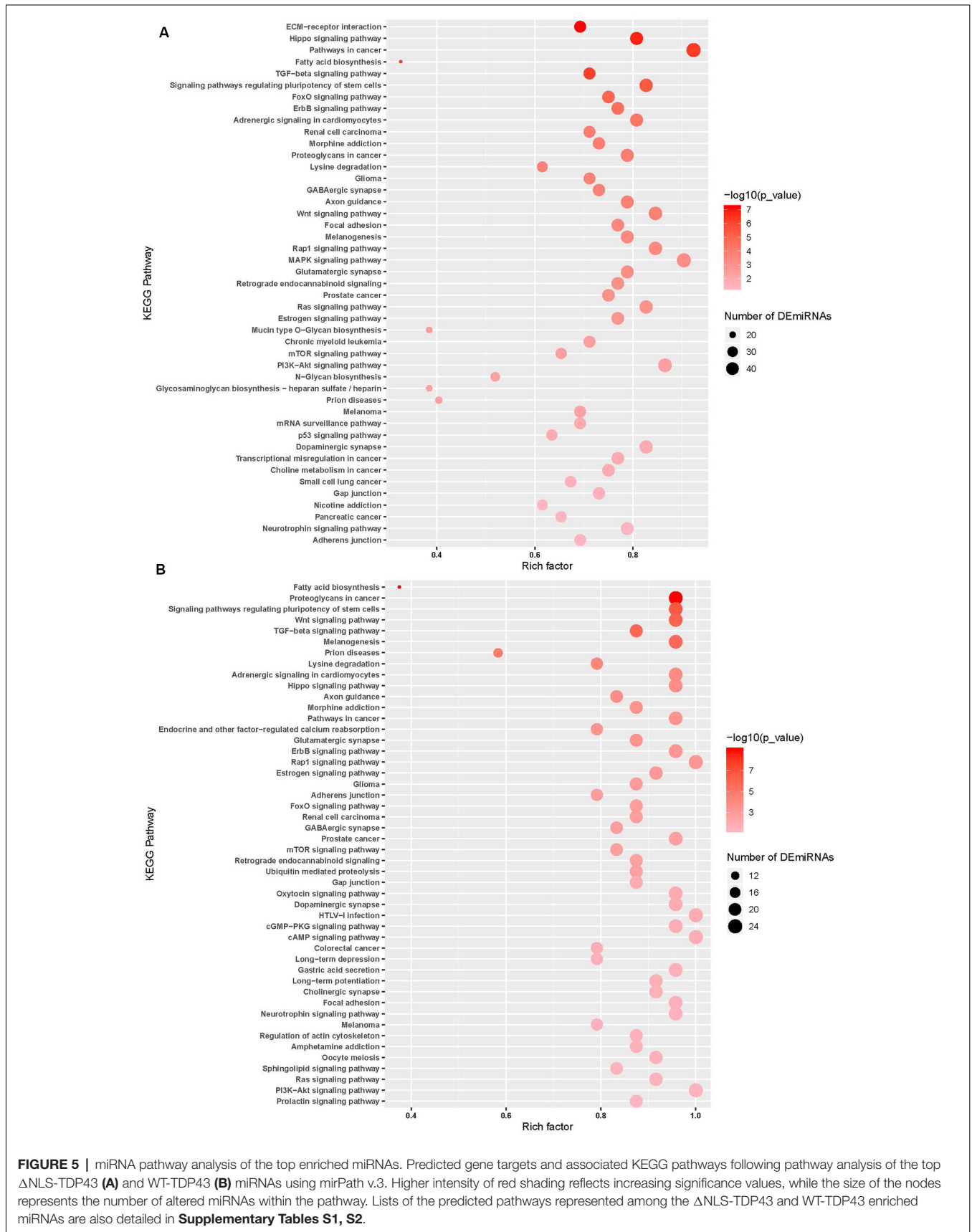


TABLE 1 | Top enriched miRNAs.

	Δ NLS-TDP43	WT-TDP43
hsa-let-7c-5p	-1.63	
hsa-miR-100-5p		-1.78
hsa-miR-10a-5p	1.40	
hsa-miR-1180-3p	2.51	
hsa-miR-1244		-4.10
hsa-miR-1246	2.39	
hsa-miR-125a-5p	-1.52	
hsa-miR-125b-5p	-1.45	
hsa-miR-126-3p	2.18	
hsa-miR-129-2-3p	5.17	
hsa-miR-129-5p	8.74	3.23
hsa-miR-1306-5p	-2.21	
hsa-miR-140-5p	1.66	
hsa-miR-148b-3p	-1.90	
hsa-miR-1537-3p	-2.62	
hsa-miR-15a-5p		1.69
hsa-miR-15b-5p	1.39	
hsa-miR-16-5p	1.64	1.78
hsa-miR-183-5p		-1.32
hsa-miR-1908-5p	1.91	
hsa-miR-192-5p		3.30
hsa-miR-196b-5p	-2.05	
hsa-miR-19a-3p	1.77	1.62
hsa-miR-19b-3p	1.80	1.83
hsa-miR-204-5p	6.50	5.56
hsa-miR-215-5p	-3.57	
hsa-miR-21-5p	1.95	
hsa-miR-221-3p		3.34
hsa-miR-23b-3p	-1.23	-1.35
hsa-miR-26b-5p	1.36	
hsa-miR-29c-3p	-2.15	
hsa-miR-301a-3p		1.80
hsa-miR-3065-5p		7.79
hsa-miR-330-5p		-3.52
hsa-miR-3605-3p	-4.51	
hsa-miR-362-3p	-1.70	
hsa-miR-362-5p	-2.16	
hsa-miR-374a-5p	-1.54	
hsa-miR-421	-2.36	
hsa-miR-450a-5p	-2.23	
hsa-miR-450b-5p	-2.30	
hsa-miR-454-3p	1.34	
hsa-miR-455-3p	1.79	
hsa-miR-486-3p	2.61	
hsa-miR-503-5p	-2.64	-1.54
hsa-miR-505-3p	2.32	
hsa-miR-532-5p	-2.25	
hsa-miR-545-3p	-4.16	
hsa-miR-548a1		-4.58
hsa-miR-548b-3p	1.71	1.50
hsa-miR-548v		-4.19
hsa-miR-550a-5p		-2.26
hsa-miR-577	15.23	9.49
hsa-miR-582-5p	-1.37	-1.38
hsa-miR-593-3p		2.76
hsa-miR-615-5p	-4.57	
hsa-miR-628-3p	-3.95	
hsa-miR-642a-5p*	3.11	1.99

(Continued)

TABLE 1 | Continued

	Δ NLS-TDP43	WT-TDP43
hsa-miR-643	2.13	
hsa-miR-651-5p	-2.81	-2.10
hsa-miR-652-3p	-2.00	
hsa-miR-660-5p	-2.14	
hsa-miR-877-5p	-6.03	
hsa-miR-99a-5p	-1.55	
hsa-miR-99b-5p	-1.60	

Bold denotes fold changes ≥ 3 ; shading indicates miRNAs altered in both cell lines.

(Neumann et al., 2006; Zhang et al., 2008; Liu-Yesucevitz et al., 2010; Davidson et al., 2016).

Importantly, since cyTDP43 pathology is present in both fALS and sALS (Hardiman et al., 2017), and even a minor increase in TDP43 levels can drive neurodegeneration (Barmada and Finkbeiner, 2010; Barmada et al., 2010; Wegorzewska and Baloh, 2011; Janssens et al., 2013; Weskamp and Barmada, 2018), miRNAs associated with cyTDP43 from either cell line could potentially provide insight into mechanisms underlying miRNA dynamics in ALS. miRNAs that interacted with cyTDP43 were assessed by NanoString profiling, an approach that enables rapid, accurate analysis of up to 800+ biologically relevant miRNAs without the need for amplification (M'Boutchou and van Kempen, 2016⁴). We identified 65 miRNAs that significantly differentially associated with cyTDP43 vs. control eGFP-His-expressing cells. As expected, cyTDP43 expression in the Δ NLS-TDP43-eGFP-His line led to a larger number of associated miRNAs ($n = 52$) than in the WT-TDP43-eGFP-His line ($n = 25$), which were increased and decreased in enrichment relative to the control cell line. Interestingly, 11 miRNAs varied by 3-fold or more, and 12 miRNAs were altered in both the WT-TDP43-eGFP-His and Δ NLS-TDP43-eGFP-His lines.

Among the most highly differentially represented miRNAs, we identified several novel miRNAs that have not previously been linked to ALS, such as miR-3065 and miR-129-5p. While little has been reported on the function of miR-3065, miR-129-5p is implicated in epilepsy (Sosanya et al., 2015; Liu et al., 2017; Rajman et al., 2017), neuroinflammation in ischemia-reperfusion (Li et al., 2017), and Alzheimer's disease (Zeng et al., 2019). Our study suggests a potential neuroprotective role for miR-129-5p, which is blocked when miR-129-5p associates with cyTDP43; however, more research is needed to fully understand the meaning of the interaction of miR-129-5p with cyTDP43.

Several of the cyTDP43-associated miRNAs we identified herein are known to have a role in ALS pathogenesis. miR-577, which was highly increased in both cells lines in our study, is predicted to target eukaryotic translation initiation factor 2C, 2/argonaute 2 (EIF2C2/AGO2), a member of the RNA-induced silencing complex (RISC), which interacts with mature miRNAs to bind mRNAs and interfere with their translation (Ha and Kim, 2014; Kobayashi and Tomari, 2016). Interestingly, miR-577 is decreased in *postmortem* sALS spinal cord tissue with a concomitant increase in EIF2C2/AGO2 gene expression

⁴<https://www.nanostring.com/products/mirna-assays>

(Figuroa-Romero et al., 2016). In parallel, we found that miR-129-2-3p was highly associated with cyTDP43 in our Δ NLS-TDP43-eGFP-His line and that miR-204-5p was increased in both lines. However, both miR-129-2-3p and miR-204-5p are lower at the neuromuscular junction of ALS subjects (De Felice et al., 2018). Finally, miR-221-3p was among the more highly enriched cy-TDP43-associated miRNAs in our study but has been reported to be both increased and decreased in other ALS studies (D'Erchia et al., 2017; Di Pietro et al., 2018; Taguchi and Wang, 2018).

The discordance between reported studies and some of our top miRNAs likely reflects that the clinical profiling studies evaluated case/control differences in plasma, blood, CSF, muscle biopsies, or spinal cord tissue (Joilin et al., 2019), while we looked more directly at miRNAs that associate with cyTDP43. It is possible that miRNAs that more highly associate with cyTDP43 may be sequestered and do not reach peripheral biofluids or tissues, and thereby are reduced in studies profiling biofluids and tissue samples. It is also plausible that miRNAs that interact with cyTDP43 earlier in the course of the disease could lead to ultimate depletion and/or compensatory changes in *postmortem* assessment.

Another confounding factor is that TDP43 autoregulates its expression levels (Ayala et al., 2011; Prasad et al., 2019). TDP43 is known to localize to stress granules under stress conditions (Emde et al., 2015; Paez-Colasante et al., 2015; Weskamp and Barmada, 2018; Chen and Cohen, 2019), and cytoplasmic TDP43 redistribution may represent a physiologic response to stress that becomes toxic if the normal distribution is not reestablished (Barmada and Finkbeiner, 2010). Thus, it is unclear if the association of certain miRNAs with cyTDP43 represents a possible preventive measure or rather promotes neuronal injury. In the case of miR-204, levels are increased in a cellular model of Parkinson's disease (Talepoor Ardakani et al., 2019), it is implicated in optic nerve injury (Wang et al., 2018), and miR-204 overexpression impairs neurite outgrowth (López-González et al., 2018) while inhibition provides neuroprotection (Yan et al., 2019). Ultimately, more research is needed to determine how miRNA profiles change over time, associate with TDP43, and impact ALS progression.

We also found an increased association of miR-15a-5p and miR-16-5p with cyTDP43. These miRNAs belong to a miR-15/16 cluster in an intronic region of the DLEU2 gene on chromosome 13 and are linked to ALS through profiling peripheral blood, neuron-derived extracellular vesicles, and muscle from ALS subjects (Liguori et al., 2018; Si et al., 2018; Katsu et al., 2019). Much of the published data on this cluster indicate that miR-15/16 members directly target the apoptosis regulator Bcl-2 to inhibit cellular proliferation, induce cancer cell apoptosis, and thereby reduce tumorigenicity (Aqeilan et al., 2010; Pekarsky et al., 2018). Since Bcl-2 is also tied to apoptotic regulation in neural cells (Azzouz et al., 2000; Soane and Fiskum, 2005; Hollville et al., 2019), similar mechanisms could be relevant to ALS. We speculate that the increased associations of miR-15/16 we observed with cyTDP43 could sequester these miRNAs, preventing Bcl-2 regulation, which in turn could promote cell death in ALS. Future studies are needed

to confirm this possibility and understand the role of miR-15/16 in ALS pathogenesis.

At the pathway level, our results overlap with reported studies. Examining predicted target pathways identified over 30 linked to both WT-TDP43-eGFP-His and Δ NLS-TDP43-eGFP-His lines, as well as several others that were represented in either cell line. While many were related to cancer signaling, pathways connected to neuronal function and health were also commonly reflected, including GABAergic and glutamatergic synapses, axon guidance, and neurotrophin signaling pathways. Moreover, our analysis identified several pathways linked to miRNA profiles identified in ALS subject muscle tissue and serum, including regulation of actin cytoskeleton, ubiquitin-mediated proteolysis, and transforming growth factor- β (TGF- β) signaling (Kovanda et al., 2018; Taguchi and Wang, 2018). The TGF- β signaling pathway is an established player in neuronal health (Barmada and Finkbeiner, 2010; Katsuno et al., 2011) and increased levels are associated with early disease stages in animal models and ALS subjects (Si et al., 2014, 2015; Meroni et al., 2019). Thus, these and other related pathways may provide important insights into the mechanisms and therapeutic opportunities for ALS.

Although the current study identified several intriguing cyTDP43-associated miRNAs and predicted pathways, we acknowledge that these data are based on an *in vitro* system with mutant cyTDP43 expression. The Δ NLS-TDP43 mutation, however, offers an important well-established strategy to model ALS and examine both disease mechanisms and resultant phenotypic consequences of cyTDP43 expression (Winton et al., 2008; Barmada et al., 2010; Miguel et al., 2011; Walker et al., 2015). Notably, *in vitro* studies using similar strategies have also verified that toxicity associated with Δ NLS-TDP43 parallels that of common TDP43 mutations seen in ALS subjects (Winton et al., 2008; Barmada et al., 2010, 2014). The overlap between our Δ NLS-TDP43 results and those from the WT-TDP43 line exhibiting moderate overexpression further supports the relevance of our observations. Future studies examining miRNA profiles that associate with cyTDP43 in relevant ALS animal models (Walker et al., 2015) and *postmortem* tissue are needed to both confirm the *in vitro* data as well as assess potential interventions based on identified targets.

We also acknowledge that cyTDP43 translocation can have implications beyond direct interactions with mature miRNAs. Our initial assessments of pri-miRNA levels for two differentially expressed mature miRNAs observed in ALS subject *postmortem* spinal cord tissue indicates that pri-miRNA expression was not altered, but that alterations must emerge at the level of miRNA processing (Figuroa-Romero et al., 2016). Other studies have also verified that TDP43 directly interacts with pri-miRNA and pre-miRNA intermediates and miRNA biosynthetic pathway components (Buratti et al., 2010; Kawahara and Mieda-Sato, 2012). Thus, while in the current study we only assessed mature miRNAs that interacted with TDP43, it is possible the impact of TDP43 may be conferred on miRNA intermediates along the biogenesis pathway or *via* sequestration in inclusions like stress granules (Emde et al., 2015; Paez-Colasante et al., 2015; Weskamp and Barmada, 2018). Future assessment of these alternative roles of cyTDP43 is needed. Finally, the

miRNAs we identified did not overlap entirely with other reported studies (Dardiotis et al., 2018). This may be due to the heterogeneity in sALS samples examined by other studies relative to our specific focus on miRNAs bound to cyTDP43 in HeLa cells.

Overall, the current study used cellular models to identify miRNAs that interact with cyTDP43. We identified known and novel dysregulated miRNAs, data that provide a foundation for inferred biological insight and potential pathomechanisms from predicted pathways. cyTDP43 inclusions, by sequestering miRNAs, may skew neuronal epigenetic homeostasis and result in motor neuron death. Our findings may therefore guide further research examining the molecular downstream events resulting from dysregulated miRNAs that influence neurodegeneration in ALS and identify new biomarkers and therapeutic targets for disease diagnosis and intervention.

DATA AVAILABILITY STATEMENT

The datasets generated for this study can be found in the Gene Expression Omnibus (GEO; <https://www.ncbi.nlm.nih.gov/geo/query/acc.cgi?acc=GSE145214>).

AUTHOR CONTRIBUTIONS

XP-C, CF-R, JH, LH, NW, SB, and EF contributed to the conception and design of the study. XP-C, CF-R, AR, FM, JMH, CB, GT, and LH contributed to the acquisition of data. XP-C and JH performed the statistical analysis. XP-C, C-FR, AR, JH,

LH, SB, SS, and EF interpreted the data. XP-C and SS wrote the first draft of the manuscript. CF-R and AR wrote sections of the manuscript. All authors contributed to manuscript revision, read, and approved the submitted version.

FUNDING

Funding support was provided by the NeuroNetwork for Emerging Therapies, the A. Alfred Taubman Medical Research Institute, the Sinai Medical Staff Foundation Neuroscience Scholar Fund, and the National Institutes of Health (F32 DK112642 and K99 DK119366 to AR; R01 GM081025 and GM062357 to NW; and R01 NS097542 to SB).

ACKNOWLEDGMENTS

We would like to thank Ms. Maegan Tabbey for assistance with protein assays, Ms. Crystal Pacut for advice generating the stable cell lines, and Dr. Masha G. Savelieff for expert editorial assistance. We would also like to thank Dr. Robert J. Kelm (University of Vermont, Burlington, VT, USA) for expert advice in optimizing the TDP43 miRNA binding ELISA.

SUPPLEMENTARY MATERIAL

The Supplementary Material for this article can be found online at: <https://www.frontiersin.org/articles/10.3389/fncel.2020.00117/full#supplementary-material>.

REFERENCES

- Aqeilan, R. I., Calin, G. A., and Croce, C. M. (2010). miR-15a and miR-16-1 in cancer: discovery, function and future perspectives. *Cell Death Differ.* 17, 215–220. doi: 10.1038/cdd.2009.69
- Archbold, H. C., Jackson, K. L., Arora, A., Weskamp, K., Tank, E. M., Li, X., et al. (2018). TDP43 nuclear export and neurodegeneration in models of amyotrophic lateral sclerosis and frontotemporal dementia. *Sci. Rep.* 8:4606. doi: 10.1038/s41598-018-22858-w
- Ayala, Y. M., De Conti, L., Avendaño-Vázquez, S. E., Dhir, A., Romano, M., D'Ambrogio, A., et al. (2011). TDP-43 regulates its mRNA levels through a negative feedback loop. *EMBO J.* 30, 277–288. doi: 10.1038/emboj.2010.310
- Ayala, Y. M., Pantano, S., D'Ambrogio, A., Buratti, E., Brindisi, A., Marchetti, C., et al. (2005). Human, *Drosophila*, and *C.elegans* TDP43: nucleic acid binding properties and splicing regulatory function. *J. Mol. Biol.* 348, 575–588. doi: 10.1016/j.jmb.2005.02.038
- Ayala, Y. M., Zago, P., D'Ambrogio, A., Xu, Y. F., Petrucelli, L., Buratti, E., et al. (2008). Structural determinants of the cellular localization and shuttling of TDP-43. *J. Cell Sci.* 121, 3778–3785. doi: 10.1242/jcs.038950
- Azzouz, M., Hottinger, A., Paterna, J. C., Zurn, A. D., Aebischer, P., and Büeler, H. (2000). Increased motoneuron survival and improved neuromuscular function in transgenic ALS mice after intraspinal injection of an adeno-associated virus encoding Bcl-2. *Hum. Mol. Genet.* 9, 803–811. doi: 10.1093/hmg/9.5.803
- Balendra, R., and Isaacs, A. M. (2018). C9orf72-mediated ALS and FTD: multiple pathways to disease. *Nat. Rev. Neurol.* 14, 544–558. doi: 10.1038/s41582-018-0047-2
- Barmada, S. J., and Finkbeiner, S. (2010). Pathogenic TARDBP mutations in amyotrophic lateral sclerosis and frontotemporal dementia: disease-associated pathways. *Rev. Neurosci.* 21, 251–272. doi: 10.1515/revneuro.2010.21.4.251
- Barmada, S. J., Ju, S., Arjun, A., Batarse, A., Archbold, H. C., Peisach, D., et al. (2015). Amelioration of toxicity in neuronal models of amyotrophic lateral sclerosis by hUPF1. *Proc. Natl. Acad. Sci. U S A* 112, 7821–7826. doi: 10.1073/pnas.1509744112
- Barmada, S. J., Serio, A., Arjun, A., Bilican, B., Daub, A., Ando, D. M., et al. (2014). Autophagy induction enhances TDP43 turnover and survival in neuronal ALS models. *Nat. Chem. Biol.* 10, 677–685. doi: 10.1038/nchembio.1563
- Barmada, S. J., Skibinski, G., Korb, E., Rao, E. J., Wu, J. Y., and Finkbeiner, S. (2010). Cytoplasmic mislocalization of TDP-43 is toxic to neurons and enhanced by a mutation associated with familial amyotrophic lateral sclerosis. *J. Neurosci.* 30, 639–649. doi: 10.1523/JNEUROSCI.4988-09.2010
- Bhardwaj, A., Myers, M. P., Buratti, E., and Baralle, F. E. (2013). Characterizing TDP-43 interaction with its RNA targets. *Nucleic Acids Res.* 41, 5062–5074. doi: 10.1093/nar/gkt189
- Birsa, N., Bentham, M. P., and Fratta, P. (2020). Cytoplasmic functions of TDP-43 and FUS and their role in ALS. *Semin. Cell Dev. Biol.* 99, 193–201. doi: 10.1016/j.semcdb.2019.05.023
- Brown, R. H., and Al-Chalabi, A. (2017). Amyotrophic lateral sclerosis. *N. Engl. J. Med.* 377, 162–172. doi: 10.1056/NEJMra1603471
- Buratti, E., De Conti, L., Stuan, C., Romano, M., Baralle, M., and Baralle, F. (2010). Nuclear factor TDP-43 can affect selected microRNA levels. *FEBS J.* 277, 2268–2281. doi: 10.1111/j.1742-4658.2010.07643.x
- Campos-Melo, D., Droppelmann, C. A., He, Z., Volkening, K., and Strong, M. J. (2013). Altered microRNA expression profile in Amyotrophic Lateral Sclerosis: a role in the regulation of NFL mRNA levels. *Mol. Brain* 6:26. doi: 10.1186/1756-6606-6-26
- Chen, Y., and Cohen, T. J. (2019). Aggregation of the nucleic acid-binding protein TDP-43 occurs via distinct routes that are coordinated with stress granule formation. *J. Biol. Chem.* 294, 3696–3706. doi: 10.1074/jbc.RA118.006351
- Chen-Plotkin, A. S., Lee, V. M., and Trojanowski, J. Q. (2010). TAR DNA-binding protein 43 in neurodegenerative disease. *Nat. Rev. Neurol.* 6, 211–220. doi: 10.1038/nrneuro.2010.18

- Chia, R., Chiò, A., and Traynor, B. J. (2018). Novel genes associated with amyotrophic lateral sclerosis: diagnostic and clinical implications. *Lancet Neurol.* 17, 94–102. doi: 10.1016/s1474-4422(17)30401-5
- Dardiotis, E., Aloizou, A. M., Stokas, V., Patrinos, G. P., Deretzi, G., Mitsias, P., et al. (2018). The role of MicroRNAs in patients with amyotrophic lateral sclerosis. *J. Mol. Neurosci.* 66, 617–628. doi: 10.1007/s12031-018-1204-1
- Davidson, Y., Robinson, A. C., Liu, X., Wu, D., Troakes, C., Rollinson, S., et al. (2016). Neurodegeneration in frontotemporal lobar degeneration and motor neurone disease associated with expansions in C9orf72 is linked to TDP-43 pathology and not associated with aggregated forms of dipeptide repeat proteins. *Neuropathol. Appl. Neurobiol.* 42, 242–254. doi: 10.1111/nan.122921
- De Felice, B., Manfellotto, F., Fiorentino, G., Annunziata, A., Biffali, E., Pannone, R., et al. (2018). Wide-ranging analysis of MicroRNA profiles in sporadic amyotrophic lateral sclerosis using next-generation sequencing. *Front. Genet.* 9:310. doi: 10.3389/fgene.2018.00310
- D'Erchia, A. M., Gallo, A., Manzari, C., Raho, S., Horner, D. S., Chiara, M., et al. (2017). Massive transcriptome sequencing of human spinal cord tissues provides new insights into motor neuron degeneration in ALS. *Sci. Rep.* 7:10046. doi: 10.1038/s41598-017-10488-7
- Di Carlo, V., Grossi, E., Laneve, P., Morlando, M., Dini Modigliani, S., Ballarino, M., et al. (2013). TDP-43 regulates the microprocessor complex activity during *in vitro* neuronal differentiation. *Mol. Neurobiol.* 48, 952–963. doi: 10.1007/s12035-013-8564-x
- Di Pietro, L., Lattanzi, W., and Bernardini, C. (2018). Skeletal muscle MicroRNAs as key players in the pathogenesis of amyotrophic lateral sclerosis. *Int. J. Mol. Sci.* 19:E1534. doi: 10.3390/ijms19051534
- Dolati, S., Marofi, F., Babaloo, Z., Aghebati-Maleki, L., Roshangar, L., Ahmadi, M., et al. (2018). Dysregulated network of miRNAs involved in the pathogenesis of multiple sclerosis. *Biomed. Pharmacother.* 104, 280–290. doi: 10.1016/j.biopha.2018.05.050
- Emde, A., Eitan, C., Liou, L. L., Libby, R. T., Rivkin, N., Magen, I., et al. (2015). Dysregulated miRNA biogenesis downstream of cellular stress and ALS-causing mutations: a new mechanism for ALS. *EMBO J.* 34, 2633–2651. doi: 10.15252/embj.201490493
- Engels, B. M., and Hutvagner, G. (2006). Principles and effects of microRNA-mediated post-transcriptional gene regulation. *Oncogene* 25, 6163–6169. doi: 10.1038/sj.onc.1209909
- Figuerola-Romero, C., Hur, J., Lunn, J. S., Paez-Colasante, X., Bender, D. E., Yung, R., et al. (2016). Expression of microRNAs in human post-mortem amyotrophic lateral sclerosis spinal cords provides insight into disease mechanisms. *Mol. Cell. Neurosci.* 71, 34–45. doi: 10.1016/j.mcn.2015.12.008
- Figuerola-Romero, C., Iñiguez-Lluhi, J. A., Stadler, J., Chang, C. R., Arnoult, D., Keller, P. J., et al. (2009). SUMOylation of the mitochondrial fission protein Drp1 occurs at multiple nonconsensus sites within the B domain and is linked to its activity cycle. *FASEB J.* 23, 3917–3927. doi: 10.1096/fj.09-136630
- Freischmidt, A., Müller, K., Ludolph, A. C., and Weishaupt, J. H. (2013). Systemic dysregulation of TDP-43 binding microRNAs in amyotrophic lateral sclerosis. *Acta Neuropathol. Commun.* 1:42. doi: 10.1186/2051-5960-1-42
- Gagliardi, D., Comi, G. P., Bresolin, N., and Corti, S. (2019). MicroRNAs as regulators of cell death mechanisms in amyotrophic lateral sclerosis. *J. Cell. Mol. Med.* 23, 1647–1656. doi: 10.1111/jcmm.13976
- Gao, J., Wang, L., Huntley, M. L., Perry, G., and Wang, X. (2018). Pathomechanisms of TDP-43 in neurodegeneration. *J. Neurochem.* 146, 7–20. doi: 10.1111/jnc.14327
- Goutman, S. A., Chen, K. S., Paez-Colasante, X., and Feldman, E. L. (2018). Emerging understanding of the genotype-phenotype relationship in amyotrophic lateral sclerosis. *Handb. Clin. Neurol.* 148, 603–623. doi: 10.1016/B978-0-444-64076-5.00039-9
- Gu, J., Chen, F., Iqbal, K., Gong, C. X., Wang, X., and Liu, F. (2017). Transactive response DNA-binding protein 43 (TDP-43) regulates alternative splicing of tau exon 10: Implications for the pathogenesis of tauopathies. *J. Biol. Chem.* 292, 10600–10612. doi: 10.1074/jbc.M117.783498
- Ha, M., and Kim, V. N. (2014). Regulation of microRNA biogenesis. *Nat. Rev. Mol. Cell Biol.* 15, 509–524. doi: 10.1038/nrm3838
- Hardiman, O., Al-Chalabi, A., Chio, A., Corr, E. M., Logroscino, G., Robberecht, W., et al. (2017). Amyotrophic lateral sclerosis. *Nat. Rev. Dis. Primers* 3:17071. doi: 10.1038/nrdp.2017.71
- Hollville, E., Romero, S. E., and Deshmukh, M. (2019). Apoptotic cell death regulation in neurons. *FEBS J.* 286, 3276–3298. doi: 10.1111/febs.14970
- Honda, D., Ishigaki, S., Iguchi, Y., Fujioka, Y., Udagawa, T., Masuda, A., et al. (2013). The ALS/FTLD-related RNA-binding proteins TDP-43 and FUS have common downstream RNA targets in cortical neurons. *FEBS Open Bio* 4, 1–10. doi: 10.1016/j.fob.2013.11.001
- Iguchi, Y., Katsuno, M., Niwa, J., Takagi, S., Ishigaki, S., Ikenaka, K., et al. (2013). Loss of TDP-43 causes age-dependent progressive motor neuron degeneration. *Brain* 136, 1371–1382. doi: 10.1093/brain/awt029
- Janssens, J., Wils, H., Kleinberger, G., Joris, G., Cuijt, I., Ceuterick-de Groote, C., et al. (2013). Overexpression of ALS-associated p.M337V human TDP-43 in mice worsens disease features compared to wild-type human TDP-43 mice. *Mol. Neurobiol.* 48, 22–35. doi: 10.1007/s12035-013-8427-5
- Jimenez-Pacheco, A., Franco, J. M., Lopez, S., Gomez-Zumaquero, J. M., Magdalena Leal-Lasarte, M., Caballero-Hernandez, D. E., et al. (2017). Epigenetic mechanisms of gene regulation in amyotrophic lateral sclerosis. *Adv. Exp. Med. Biol.* 978, 255–275. doi: 10.1007/978-3-319-53889-1_14
- Jobe, E. M., McQuate, A. L., and Zhao, X. (2012). Crosstalk among epigenetic pathways regulates neurogenesis. *Front. Neurosci.* 6:59. doi: 10.3389/fnins.2012.00059
- Joilin, G., Leigh, P. N., Newbury, S. F., and Hafezparast, M. (2019). An overview of MicroRNAs as biomarkers of ALS. *Front. Neurol.* 10:186. doi: 10.3389/fneur.2019.00186
- Kapeli, K., Martinez, F. J., and Yeo, G. W. (2017). Genetic mutations in RNA-binding proteins and their roles in ALS. *Hum. Genet.* 136, 1193–1214. doi: 10.1007/s00439-017-1830-7
- Katsu, M., Hama, Y., Utsumi, J., Takashina, K., Yasumatsu, H., Mori, F., et al. (2019). MicroRNA expression profiles of neuron-derived extracellular vesicles in plasma from patients with amyotrophic lateral sclerosis. *Neurosci. Lett.* 708:134176. doi: 10.1016/j.neulet.2019.03.048
- Katsuno, M., Adachi, H., Banno, H., Suzuki, K., Tanaka, F., and Sobue, G. (2011). Transforming growth factor- β signaling in motor neuron diseases. *Curr. Mol. Med.* 11, 48–56. doi: 10.2174/156652411794474356
- Kawahara, Y., and Mieda-Sato, A. (2012). TDP-43 promotes microRNA biogenesis as a component of the Drosha and Dicer complexes. *Proc. Natl. Acad. Sci. U S A* 109, 3347–3352. doi: 10.1073/pnas.1112427109
- King, I., Yartseva, V., Salas, D., Kumar, A., Heidersbach, A., Ando, D. M., et al. (2014). The RNA binding protein TDP-43 selectively disrupts MicroRNA-1/206 incorporation into the RNA-induced silencing complex. *J. Biol. Chem.* 289, 14263–14271. doi: 10.1074/jbc.M114.561902
- Kobayashi, H., and Tomari, Y. (2016). RISC assembly: coordination between small RNAs and Argonaute proteins. *Biochim. Biophys. Acta* 1859, 71–81. doi: 10.1016/j.bbargm.2015.08.007
- Kovanda, A., Leonardis, L., Zidar, J., Koritnik, B., Dolenc-Groselj, L., Ristic Kovacic, S., et al. (2018). Differential expression of microRNAs and other small RNAs in muscle tissue of patients with ALS and healthy age-matched controls. *Sci. Rep.* 8:5609. doi: 10.1038/s41598-018-23139-2
- Kwiatkowski, T. J. Jr., Bosco, D. A., Leclerc, A. L., Tamrazian, E., Vanderburg, C. R., Russ, C., et al. (2009). Mutations in the FUS/TLN3 gene on chromosome 16 cause familial amyotrophic lateral sclerosis. *Science* 323, 1205–1208. doi: 10.1126/science.1166066
- Lagos-Quintana, M., Rauhut, R., Lendeckel, W., and Tuschl, T. (2001). Identification of novel genes coding for small expressed RNAs. *Science* 294, 853–858. doi: 10.1126/science.1064921
- Lau, N. C., Lim, L. P., Weinstein, E. G., and Bartel, D. P. (2001). An abundant class of tiny RNAs with probable regulatory roles in *Caenorhabditis elegans*. *Science* 294, 858–862. doi: 10.1126/science.1065062
- Lee, R. C., and Ambros, V. (2001). An extensive class of small RNAs in *Caenorhabditis elegans*. *Science* 294, 862–864. doi: 10.1126/science.1065329
- Li, X. Q., Chen, F. S., Tan, W. F., Fang, B., Zhang, Z. L., and Ma, H. (2017). Elevated microRNA-129-5p level ameliorates neuroinflammation and blood-spinal cord barrier damage after ischemia-reperfusion by inhibiting HMGB1 and the TLR3-cytokine pathway. *J. Neuroinflammation* 14:205. doi: 10.1186/s12974-017-0977-4

- Li, Q., Yokoshi, M., Okada, H., and Kawahara, Y. (2015). The cleavage pattern of TDP-43 determines its rate of clearance and cytotoxicity. *Nat. Commun.* 6:6183. doi: 10.1038/ncomms7183
- Liguori, M., Nuzziello, N., Introna, A., Consiglio, A., Licciulli, F., D'Errico, E., et al. (2018). Dysregulation of MicroRNAs and target genes networks in peripheral blood of patients with sporadic amyotrophic lateral sclerosis. *Front. Mol. Neurosci.* 11:288. doi: 10.3389/fnmol.2018.00288
- Ling, S. C., Albuquerque, C. P., Han, J. S., Lagier-Tourenne, C., Tokunaga, S., Zhou, H., et al. (2010). ALS-associated mutations in TDP-43 increase its stability and promote TDP-43 complexes with FUS/TLS. *Proc. Natl. Acad. Sci. U S A* 107, 13318–13323. doi: 10.1073/pnas.1008227107
- Liu, A. H., Wu, Y. T., and Wang, Y. P. (2017). MicroRNA-129-5p inhibits the development of autoimmune encephalomyelitis-related epilepsy by targeting HMGB1 through the TLR4/NF- κ B signaling pathway. *Brain Res. Bull.* 132, 139–149. doi: 10.1016/j.brainresbull.2017.05.004
- Liu-Yesucevitz, L., Bilgutay, A., Zhang, Y. J., Vanderweyde, T., Citro, A., Mehta, T., et al. (2010). Tar DNA binding protein-43 (TDP-43) associates with stress granules: analysis of cultured cells and pathological brain tissue. *PLoS One* 5:e13250. doi: 10.1371/journal.pone.0013250
- Loffreda, A., Rigamonti, A., Barabino, S. M., and Lenzken, S. C. (2015). RNA-binding proteins in the regulation of miRNA activity: a focus on neuronal functions. *Biomolecules* 5, 2363–2387. doi: 10.3390/biom5042363
- López-González, M. J., Soula, A., Landry, M., and Favreux, A. (2018). Oxaliplatin treatment impairs extension of sensory neuron neurites *in vitro* through miR-204 overexpression. *Neurotoxicology* 68, 91–100. doi: 10.1016/j.neuro.2018.07.009
- Lunn, J. S., Sakowski, S. A., Kim, B., Rosenberg, A. A., and Feldman, E. L. (2009). Vascular endothelial growth factor prevents G93A-SOD1-induced motor neuron degeneration. *Dev. Neurobiol.* 69, 871–884. doi: 10.1002/dneu.20747
- Maoz, R., Garfinkel, B. P., and Soreq, H. (2017). Alzheimer's disease and ncRNAs. *Adv. Exp. Med. Biol.* 978, 337–361. doi: 10.1007/978-3-319-53889-1_18
- M'Boutchou, M. N., and van Kempen, L. C. (2016). Analysis of the tumor microenvironment transcriptome *via* NanoString mRNA and miRNA expression profiling. *Methods Mol. Biol.* 1458, 291–310. doi: 10.1007/978-1-4939-3801-8_21
- Meroni, M., Crippa, V., Cristofani, R., Rusmini, P., Cicardi, M. E., Messi, E., et al. (2019). Transforming growth factor β 1 signaling is altered in the spinal cord and muscle of amyotrophic lateral sclerosis mice and patients. *Neurobiol. Aging* 82, 48–59. doi: 10.1016/j.neurobiolaging.2019.07.001
- Miguel, L., Frebourg, T., Campion, D., and Lecourtis, M. (2011). Both cytoplasmic and nuclear accumulations of the protein are neurotoxic in *Drosophila* models of TDP-43 proteinopathies. *Neurobiol. Dis.* 41, 398–406. doi: 10.1016/j.nbd.2010.10.007
- Neumann, M., Kwong, L. K., Lee, E. B., Kremmer, E., Flatley, A., Xu, Y., et al. (2009). Phosphorylation of S409/410 of TDP-43 is a consistent feature in all sporadic and familial forms of TDP-43 proteinopathies. *Acta Neuropathol.* 117, 137–149. doi: 10.1007/s00401-008-0477-9
- Neumann, M., Sampathu, D. M., Kwong, L. K., Truax, A. C., Micsenyi, M. C., Chou, T. T., et al. (2006). Ubiquitinated TDP-43 in frontotemporal lobar degeneration and amyotrophic lateral sclerosis. *Science* 314, 130–133. doi: 10.1126/science.1134108
- Oskarsson, B., Gendron, T. F., and Staff, N. P. (2018). Amyotrophic lateral sclerosis: an update for 2018. *Mayo Clin. Proc.* 93, 1617–1628. doi: 10.1016/j.mayocp.2018.04.007
- Paez-Colasante, X., Figueroa-Romero, C., Sakowski, S. A., Goutman, S. A., and Feldman, E. L. (2015). Amyotrophic lateral sclerosis: mechanisms and therapeutics in the epigenomic era. *Nat. Rev. Neurol.* 11, 266–279. doi: 10.1038/nrneurol.2015.57
- Pekarsky, Y., Balatti, V., and Croce, C. M. (2018). BCL2 and miR-15/16: from gene discovery to treatment. *Cell Death Differ.* 25, 21–26. doi: 10.1038/cdd.2017.159
- Poddar, S., Kesharwani, D., and Datta, M. (2017). Interplay between the miRNome and the epigenetic machinery: implications in health and disease. *J. Cell Physiol.* 232, 2938–2945. doi: 10.1002/jcp.25819
- Prasad, A., Bharathi, V., Sivalingam, V., Girdhar, A., and Patel, B. K. (2019). Molecular mechanisms of TDP-43 misfolding and pathology in amyotrophic lateral sclerosis. *Front. Mol. Neurosci.* 12:25. doi: 10.3389/fnmol.2019.00025
- Quinlan, S., Kenny, A., Medina, M., Engel, T., and Jimenez-Mateos, E. M. (2017). MicroRNAs in Neurodegenerative Diseases. *Int Rev Cell Mol Biol* 334, 309–343. doi: 10.1016/bs.ircmb.2017.04.002
- Rajman, M., Metge, F., Fiore, R., Khudayberdiev, S., Aksoy-Aksel, A., Bicker, S., et al. (2017). A microRNA-129-5p/Rbfox crosstalk coordinates homeostatic downscaling of excitatory synapses. *EMBO J.* 36, 1770–1787. doi: 10.15252/embj.201695748
- Ramsey, J. E., and Kelm, R. J. Jr. (2009). Mechanism of strand-specific smooth muscle α -actin enhancer interaction by purine-rich element binding protein B (Pur β). *Biochemistry* 48, 6348–6360. doi: 10.1021/bi900708j
- Rinchetti, P., Rizzuti, M., Faravelli, I., and Corti, S. (2018). MicroRNA metabolism and dysregulation in amyotrophic lateral sclerosis. *Mol. Neurobiol.* 55, 2617–2630. doi: 10.1007/s12035-017-0537-z
- Rumora, A. E., Steere, A. N., Ramsey, J. E., Knapp, A. M., Ballif, B. A., and Kelm, R. J. Jr. (2010). Isolation and characterization of the core single-stranded DNA-binding domain of purine-rich element binding protein B (Pur β). *Biochem. Biophys. Res. Commun.* 400, 340–345. doi: 10.1016/j.bbrc.2010.08.059
- Rumora, A. E., Wang, S. X., Ferris, L. A., Everse, S. J., and Kelm, R. J. Jr. (2013). Structural basis of multisite single-stranded DNA recognition and ACTA2 repression by purine-rich element binding protein B (Pur β). *Biochemistry* 52, 4439–4450. doi: 10.1021/bi400283r
- Ryan, J. A. (2008). *Cell Cloning by Serial Dilution in 96 Well Plates Protocol*. Corning, NY: Corning Incorporated. Available online at: https://www.corning.com/catalog/cls/documents/protocols/Single_cell_cloning_protocol.pdf.
- Selbach, M., Schwanhauser, B., Thierfelder, N., Fang, Z., Khanin, R., and Rajewsky, N. (2008). Widespread changes in protein synthesis induced by microRNAs. *Nature* 455, 58–63. doi: 10.1038/nature07228
- Sephton, C. F., Cenik, C., Kucukural, A., Dammer, E. B., Cenik, B., Han, Y., et al. (2011). Identification of neuronal RNA targets of TDP-43-containing ribonucleoprotein complexes. *J. Biol. Chem.* 286, 1204–1215. doi: 10.1074/jbc.M110.190884
- Sephton, C. F., Good, S. K., Atkin, S., Dewey, C. M., Mayer, P. III., Herz, J., et al. (2010). TDP-43 is a developmentally regulated protein essential for early embryonic development. *J. Biol. Chem.* 285, 6826–6834. doi: 10.1074/jbc.M109.061846
- Sharma, S., De Carvalho, D. D., Jeong, S., Jones, P. A., and Liang, G. (2011). Nucleosomes containing methylated DNA stabilize DNA methyltransferases 3A/3B and ensure faithful epigenetic inheritance. *PLoS Genet.* 7:e1001286. doi: 10.1371/journal.pgen.1001286
- Si, Y., Cui, X., Crossman, D. K., Hao, J., Kazamel, M., Kwon, Y., et al. (2018). Muscle microRNA signatures as biomarkers of disease progression in amyotrophic lateral sclerosis. *Neurobiol. Dis.* 114, 85–94. doi: 10.1016/j.nbd.2018.02.009
- Si, Y., Cui, X., Kim, S., Wians, R., Sorge, R., Oh, S. J., et al. (2014). Smads as muscle biomarkers in amyotrophic lateral sclerosis. *Ann. Clin. Transl. Neurol.* 1, 778–787. doi: 10.1002/acn3.117
- Si, Y., Kim, S., Cui, X., Zheng, L., Oh, S. J., Anderson, T., et al. (2015). Transforming growth factor β (TGF- β) is a muscle biomarker of disease progression in ALS and correlates with smad expression. *PLoS One* 10:e0138425. doi: 10.1371/journal.pone.0138425
- Singh, A., and Sen, D. (2017). MicroRNAs in Parkinson's disease. *Exp. Brain Res.* 235, 2359–2374. doi: 10.1007/s00221-017-4989-1
- Soane, L., and Fiskum, G. (2005). Inhibition of mitochondrial neural cell death pathways by protein transduction of Bcl-2 family proteins. *J. Bioenerg. Biomembr.* 37, 179–190. doi: 10.1007/s10863-005-6590-8
- Sosanya, N. M., Brager, D. H., Wolfe, S., Niere, F., and Raab-Graham, K. F. (2015). Rapamycin reveals an mTOR-independent repression of Kv1.1 expression during epileptogenesis. *Neurobiol. Dis.* 73, 96–105. doi: 10.1016/j.nbd.2014.09.011
- Spiller, K. J., Cheung, C. J., Restrepo, C. R., Kwong, L. K., Stieber, A. M., Trojanowski, J. Q., et al. (2016a). Selective motor neuron resistance and recovery in a new inducible mouse model of TDP-43 proteinopathy. *J. Neurosci.* 36, 7707–7717. doi: 10.1523/jneurosci.1457-16.2016
- Spiller, K. J., Restrepo, C. R., Khan, T., Stieber, A. M., Kwong, L. K., Trojanowski, J. Q., et al. (2016b). Progression of motor neuron disease is

- accelerated and the ability to recover is compromised with advanced age in rNLS8 mice. *Acta Neuropathol. Commun.* 4:105. doi: 10.1186/s40478-016-0377-5
- Spiller, K. J., Khan, T., Dominique, M. A., Restrepo, C. R., Cotton-Samuel, D., Levitan, M., et al. (2019). Reduction of matrix metalloproteinase 9 (MMP-9) protects motor neurons from TDP-43-triggered death in rNLS8 mice. *Neurobiol. Dis.* 124, 133–140. doi: 10.1016/j.nbd.2018.11.013
- Spiller, K. J., Restrepo, C. R., Khan, T., Dominique, M. A., Fang, T. C., Canter, R. G., et al. (2018). Microglia-mediated recovery from ALS-relevant motor neuron degeneration in a mouse model of TDP-43 proteinopathy. *Nat. Neurosci.* 21, 329–340. doi: 10.1038/s41593-018-0083-7
- Sreedharan, J., Blair, I. P., Tripathi, V. B., Hu, X., Vance, C., Rogelj, B., et al. (2008). TDP-43 mutations in familial and sporadic amyotrophic lateral sclerosis. *Science* 319, 1668–1672. doi: 10.1126/science.1154584
- Taguchi, Y. H., and Wang, H. (2018). Exploring microRNA biomarker for amyotrophic lateral sclerosis. *Int. J. Mol. Sci.* 19:E1318. doi: 10.3390/ijms19051318
- Takahashi, I., Hama, Y., Matsushima, M., Hirotsu, M., Kano, T., Hohzen, H., et al. (2015). Identification of plasma microRNAs as a biomarker of sporadic Amyotrophic Lateral Sclerosis. *Mol. Brain* 8:67. doi: 10.1186/s13041-015-0161-7
- Talepoor Ardakani, M., Rostamian Delavar, M., Baghi, M., Nasr-Esfahani, M. H., Kiani-Esfahani, A., and Ghaedi, K. (2019). Upregulation of miR-200a and miR-204 in MPP⁺-treated differentiated PC12 cells as a model of Parkinson's disease. *Mol. Genet. Genomic Med.* 7:e548. doi: 10.1002/mgg3.548
- Tan, L., Yu, J. T., and Tan, L. (2015). Causes and consequences of MicroRNA dysregulation in neurodegenerative diseases. *Mol. Neurobiol.* 51, 1249–1262. doi: 10.1007/s12035-014-8803-9
- Vance, C., Rogelj, B., Hortobagyi, T., De Vos, K. J., Nishimura, A. L., Sreedharan, J., et al. (2009). Mutations in FUS, an RNA processing protein, cause familial amyotrophic lateral sclerosis type 6. *Science* 323, 1208–1211. doi: 10.1126/science.1165942
- Vlachos, I. S., Zagganas, K., Paraskevopoulou, M. D., Georgakilas, G., Karagkouni, D., Vergoulis, T., et al. (2015). DIANA-miRPath v3.0: deciphering microRNA function with experimental support. *Nucleic Acids Res.* 43, W460–W466. doi: 10.1093/nar/gkv403
- Vucic, S., Rothstein, J. D., and Kiernan, M. C. (2014). Advances in treating amyotrophic lateral sclerosis: insights from pathophysiological studies. *Trends Neurosci.* 37, 433–442. doi: 10.1016/j.tins.2014.05.006
- Walker, A. K., Spiller, K. J., Ge, G., Zheng, A., Xu, Y., Zhou, M., et al. (2015). Functional recovery in new mouse models of ALS/FTLD after clearance of pathological cytoplasmic TDP-43. *Acta Neuropathol.* 130, 643–660. doi: 10.1007/s00401-015-1460-x
- Wang, N., Yang, W., Xiao, T., Miao, Z., Luo, W., You, Z., et al. (2018). Possible role of miR-204 in optic nerve injury through the regulation of GAP-43. *Mol. Med. Rep.* 17, 3891–3897. doi: 10.3892/mmr.2017.8341
- Wang, X., Zhou, S., Ding, X., Ma, M., Zhang, J., Zhou, Y., et al. (2015). Activation of ER stress and autophagy induced by TDP-43 A315T as pathogenic mechanism and the corresponding histological changes in skin as potential biomarker for ALS with the mutation. *Int. J. Biol. Sci.* 11, 1140–1149. doi: 10.7150/ijbs.12657
- Wegorzewska, I., and Baloh, R. H. (2011). TDP-43-based animal models of neurodegeneration: new insights into ALS pathology and pathophysiology. *Neurodegener. Dis.* 8, 262–274. doi: 10.1159/000321547
- Weskamp, K., and Barmada, S. J. (2018). TDP43 and RNA instability in amyotrophic lateral sclerosis. *Brain Res.* 1693, 67–74. doi: 10.1016/j.brainres.2018.01.015
- Weskamp, K., Tank, E. M., Miguez, R., McBride, J. P., Gomez, N. B., White, M., et al. (2020). Shortened TDP43 isoforms upregulated by neuronal hyperactivity drive TDP43 pathology in ALS. *J. Clin. Invest.* 130, 1139–1155. doi: 10.1172/JCI130988
- Wils, H., Kleinberger, G., Janssens, J., Pereson, S., Joris, G., Cuijt, I., et al. (2010). TDP-43 transgenic mice develop spastic paralysis and neuronal inclusions characteristic of ALS and frontotemporal lobar degeneration. *Proc. Natl. Acad. Sci. U S A* 107, 3858–3863. doi: 10.1073/pnas.0912417107
- Winton, M. J., Igaz, L. M., Wong, M. M., Kwong, L. K., Trojanowski, J. Q., and Lee, V. M. (2008). Disturbance of nuclear and cytoplasmic TAR DNA-binding protein (TDP-43) induces disease-like redistribution, sequestration, and aggregate formation. *J. Biol. Chem.* 283, 13302–13309. doi: 10.1074/jbc.m800342200
- Wohlfarth, C., Schmitteckert, S., Hartle, J. D., Houghton, L. A., Dweep, H., Fortea, M., et al. (2017). miR-16 and miR-103 impact 5-HT₄ receptor signalling and correlate with symptom profile in irritable bowel syndrome. *Sci. Rep.* 7:14680. doi: 10.1038/s41598-017-13982-0
- Yan, L., Shi, E., Jiang, X., Shi, J., Gao, S., and Liu, H. (2019). Inhibition of MicroRNA-204 conducts neuroprotection against spinal cord ischemia. *Ann. Thorac. Surg.* 107, 76–83. doi: 10.1016/j.athoracsur.2018.07.082
- Zeng, Z., Liu, Y., Zheng, W., Liu, L., Yin, H., Zhang, S., et al. (2019). MicroRNA-129-5p alleviates nerve injury and inflammatory response of Alzheimer's disease via downregulating SOX6. *Cell Cycle* 18, 3095–3110. doi: 10.1080/15384101.2019.1669388
- Zhang, H., Tan, C. F., Mori, F., Tanji, K., Kakita, A., Takahashi, H., et al. (2008). TDP-43-immunoreactive neuronal and glial inclusions in the neostriatum in amyotrophic lateral sclerosis with and without dementia. *Acta Neuropathol.* 115, 115–122. doi: 10.1007/s00401-007-0285-7

Conflict of Interest: EF consulted for Novartis in 2019.

The remaining authors declare that the research was conducted in the absence of any commercial or financial relationships that could be construed as a potential conflict of interest.

Copyright © 2020 Paez-Colasante, Figueroa-Romero, Rumora, Hur, Mendelson, Hayes, Backus, Taubman, Heinicke, Walter, Barmada, Sakowski and Feldman. This is an open-access article distributed under the terms of the Creative Commons Attribution License (CC BY). The use, distribution or reproduction in other forums is permitted, provided the original author(s) and the copyright owner(s) are credited and that the original publication in this journal is cited, in accordance with accepted academic practice. No use, distribution or reproduction is permitted which does not comply with these terms.

Supplementary Material

Supplementary Table 1. Predicted pathways represented among the ΔNLS-TDP43 enriched miRNAs (n=52)			
KEGG pathway	p-value	#genes	#miRNAs
ECM-receptor interaction	6.70E-08	47	36
Hippo signaling pathway	1.53E-07	99	42
Pathways in cancer	4.95E-07	243	48
Fatty acid biosynthesis	7.06E-07	8	17
TGF-beta signaling pathway	7.06E-07	55	37
Signaling pathways regulating pluripotency of stem cells	3.98E-06	93	43
FoxO signaling pathway	1.34E-05	91	39
ErbB signaling pathway	2.77E-05	63	40
Adrenergic signaling in cardiomyocytes	5.74E-05	93	42
Renal cell carcinoma	0.000107141	47	37
Morphine addiction	0.000107141	59	38
Proteoglycans in cancer	0.000107141	121	41
Lysine degradation	0.000163457	31	32
Glioma	0.000163457	44	37
GABAergic synapse	0.000163457	54	38
Axon guidance	0.000163457	83	41
Wnt signaling pathway	0.00016376	90	44
Focal adhesion	0.000295871	129	40
Melanogenesis	0.000390693	67	41
Rap1 signaling pathway	0.000390693	130	44
MAPK signaling pathway	0.000532291	155	47
Glutamatergic synapse	0.000583187	70	41
Retrograde endocannabinoid signaling	0.000752707	66	40
Prostate cancer	0.000843156	60	39
Ras signaling pathway	0.000863633	133	43
Estrogen signaling pathway	0.001231848	60	40
Mucin type O-Glycan biosynthesis	0.00262994	17	20
Chronic myeloid leukemia	0.003128637	50	37
mTOR signaling pathway	0.003261009	43	34
PI3K-Akt signaling pathway	0.003596696	194	45
N-Glycan biosynthesis	0.003710123	27	27
Glycosaminoglycan biosynthesis - heparan sulfate / heparin	0.00396943	17	20
Prion diseases	0.00396943	13	21
Melanoma	0.004724066	49	36
mRNA surveillance pathway	0.012225822	57	36
p53 signaling pathway	0.012646318	45	33
Dopaminergic synapse	0.012847181	80	43
Transcriptional misregulation in cancer	0.013178554	99	40
Choline metabolism in cancer	0.013783845	66	39
Small cell lung cancer	0.025902308	54	35
Gap junction	0.027321655	54	38
Nicotine addiction	0.040187853	24	32
Pancreatic cancer	0.040845619	42	34
Neurotrophin signaling pathway	0.040926583	74	41
Adherens junction	0.042366264	51	36
<i>Shading indicates pathways altered in both cell lines</i>			

Supplementary Table 2. Predicted pathways represented among the WT-TDP43 enriched miRNAs (n=24)			
KEGG pathway	p-value	#genes	#miRNAs
Fatty acid biosynthesis	1.12E-09	7	9
Proteoglycans in cancer	1.15E-09	109	23
Signaling pathways regulating pluripotency of stem cells	2.44E-07	78	23
Wnt signaling pathway	7.44E-07	79	23
TGF-beta signaling pathway	1.61E-06	45	21
Melanogenesis	1.61E-06	61	23
Prion diseases	1.34E-05	12	14
Lysine degradation	6.71E-05	26	19
Adrenergic signaling in cardiomyocytes	0.000136733	75	23
Hippo signaling pathway	0.000174349	81	23
Axon guidance	0.000186197	68	20
Morphine addiction	0.000353656	47	21
Pathways in cancer	0.000353656	187	23
Endocrine and other factor-regulated calcium reabsorption	0.000370753	25	19
Glutamatergic synapse	0.00040103	59	21
ErbB signaling pathway	0.00057494	52	23
Rap1 signaling pathway	0.00061741	106	24
Estrogen signaling pathway	0.000832107	49	22
Glioma	0.001258677	35	21
Adherens junction	0.001363224	44	19
FoxO signaling pathway	0.00138805	69	21
Renal cell carcinoma	0.001536942	39	21
GABAergic synapse	0.001609039	43	20
Prostate cancer	0.001791377	49	23
mTOR signaling pathway	0.001795883	37	20
Retrograde endocannabinoid signaling	0.00236326	52	21
Ubiquitin mediated proteolysis	0.002396717	73	21
Gap junction	0.009533856	42	21
Oxytocin signaling pathway	0.010546071	79	23
Dopaminergic synapse	0.010772117	67	23
HTLV-I infection	0.011630862	121	24
cGMP-PKG signaling pathway	0.014643481	80	23
cAMP signaling pathway	0.015042354	94	24
Colorectal cancer	0.018017609	35	19
Long-term depression	0.020363348	32	19
Gastric acid secretion	0.020363348	40	23
Long-term potentiation	0.021102204	37	22
Cholinergic synapse	0.024109204	58	22
Focal adhesion	0.024454173	96	23
Neurotrophin signaling pathway	0.024867506	61	23
Melanoma	0.025760052	38	19
Regulation of actin cytoskeleton	0.027442021	100	21
Amphetamine addiction	0.027442021	33	21
Oocyte meiosis	0.027500726	58	22
Sphingolipid signaling pathway	0.034385726	57	20
Ras signaling pathway	0.034385726	100	22
PI3K-Akt signaling pathway	0.034385726	147	24
Prolactin signaling pathway	0.048988319	35	21

Shading indicates pathways altered in both cell lines